Palaeogeography, Palaeoclimatology, Palaeoecology 679 (2025) 113266

Contents lists available at ScienceDirect

Palaeogeography, Palaeoclimatology, Palaeoecology

journal homepage: www.elsevier.com/locate/palaeo

Census collection of two fossil plant localities in Jameson Land, East Greenland supports regional ecological turnover and diversity loss at the end-Triassic mass extinction

Antonietta B. Knetge [a,*], Catarina Barbosa [a], William J. Matthaeus [a], Richard S. Barclay [e], Ian J. Glasspool [i], Bernard Gomez [f], Stephen P. Hesselbo [c], Mihai E. Popa [d], Micha Ruhl [b], David Sunderlin [g], Finn Surlyk [h], Jennifer C. McElwain [a]

[a] School of Natural Sciences, Botany, Trinity College Dublin, College Green Dublin 2, Dublin, Ireland
[b] School of Natural Sciences, Geology, Trinity College Dublin, College Green Dublin 2, Dublin, Ireland
[c] Camborne School of Mines, Department of Earth and Environmental Sciences, University of Exeter, Penryn TR10 9FE, UK
[d] Doctoral School of Geology, Faculty of Geology and Geophysics, University of Bucharest, Bucharest, Romania
[e] Department of Paleobiology, National Museum of Natural History, Smithsonian Institution, Washington, DC, USA
[f] CNRS-UMR 5276 Terre, Planètes, Environnement, Université Lyon 1, 2, rue Raphaël Dubois, F-69622 Villeurbanne, France
[g] Department of Geology and Environmental Geosciences, Lafayette College, Easton, PA 18042, USA
[h] Department of Geosciences and Natural Resource Management, University of Copenhagen, Øster Voldgade 10, 1350 Copenhagen K, Denmark
[i] Field Museum of Natural History, Chicago, IL 60605, USA

ARTICLE INFO

Editor: H Falcon-Lang

Keywords:
Palaeoecology
Taphonomy
Mass extinction event
Triassic–Jurassic

ABSTRACT

The Astartekløft field locality in Jameson Land, East Greenland shows extensive macrofloristic (>80 % of species) and palynological turnover at the end-Triassic mass extinction event, coincident with global turnover in both terrestrial and marine ecosystems. Stable carbon isotope data and the palynological record support a transitional interval between the uppermost Rhaetian and lowermost Hettangian.

A new census-collected fossil flora from South Tancrediakløft (Jameson Land Basin, East Greenland) contains 2369 well-preserved leaf specimens of 27 unique morphogenera, ranging across seven fossiliferous beds containing a Triassic–Jurassic transition zone. South Tancrediakløft floristic relative abundance data are compared with those from Astartekløft to investigate the nature and spatial extent of floristic turnover and vegetation dynamics across the Jameson Land Basin. The two sites were analysed using directly equivalent palaeoecological data sets and measures of biodiversity (evenness and richness), in conjunction with a new stable isotope stratigraphy and locality taphonomy, to assess ecological shifts across the end-Triassic event preserved in the Kap Stewart Group.

Our study demonstrates a floristic turnover occurring before the established transition and before the 'main' negative stable carbon isotope anomaly correlated to St Audrie's Bay (UK). Further, these new data indicate a 54 % genus-level loss of floristic biodiversity, loss of the lower and mid-canopy habits before the onset of the Jurassic, and a homogenised Jurassic recovery flora. Evidence of a Rhaetian fern spike and compositional evenness in the Hettangian, support a complex biphasic disturbance pattern. This comparison of localities shows the magnitude of diversity loss scales with the pre-crisis standing diversity.

1. Introduction

The end-Triassic mass extinction event (ETME) is one of the five major Phanerozoic disturbances (McGhee et al., 2004), resulting in distinct change in both terrestrial and marine ecosystems (McElwain et al., 1999; Pálfy et al., 2000; Hesselbo et al., 2002; Olsen et al., 2002; McElwain et al., 2007; Van De Schootbrugge et al., 2009; Lindstrom et al., 2012; Li et al., 2020). The main driver of the event was Central Atlantic Magmatic Province (CAMP) volcanism, which caused extensive degassing of CO_2, SO_2, CH_4 and Hg and triggered significant

* Corresponding author.
E-mail address: knetgea@tcd.ie (A.B. Knetge).

https://doi.org/10.1016/j.palaeo.2025.113266
Received 20 June 2025; Received in revised form 4 September 2025; Accepted 4 September 2025
Available online 6 September 2025

environmental change that likely impacted terrestrial biomes (Deenen et al., 2010; Schoene et al., 2010; Ruhl et al., 2010, 2011; Davies et al., 2017; Percival et al., 2017; Capriolo et al., 2020, 2021). Large carbon release into marine systems during CAMP emplacement is correlated to elevated atmospheric pCO_2 and increased oceanic and global temperatures (McElwain et al., 1999; Steinthorsdottir et al., 2011; Schaller et al., 2011; Schaller et al., 2012), and resulted in the production of thermogenic methane (Marzoli et al., 2018; Ruhl and Kürschner, 2011; Ruhl et al., 2011). CAMP driven environmental change contributed to the extinction of groups of ammonoids and conodonts, and to declines in other marine invertebrate clades (Hallam and Wignall, 1999; Mander and Twitchett, 2008; Mander et al., 2008; McGhee et al., 2004; Bond et al., 2022). Marine and continental biostratigraphy suggest CAMP volcanicity occurred in two phases (Wignall and Atkinson, 2020) with the initial pulse causing the majority of the biotic crises (Lindström, 2021).

Northern hemispheric Triassic–Jurassic macrofloristic and palynological data demonstrate a marked terrestrial vegetation response; palynological data from China's Sichuan Basin support species turnover and a fern spike (Li et al., 2020; Zhou et al., 2021). Major turnovers were observed in palynological (>80 % decline in species) and macrofloristic (35 % decline in genera) assemblages of East Greenland and Sweden; the extinction of *Lepidopteris ottonis* and its replacement by *Thaumatopteris brauniana* demarcate the respective Upper Triassic and Lower Jurassic biozones (Harris, 1937; Lundblad, 1959; Pedersen and Lund, 1980; McElwain et al., 2007; Mander et al., 2010; Kustatscher et al., 2018).

Extensive palynological analyses of the ETME interval at both Jameson Land (Pedersen and Lund, 1980; Mander et al., 2010, 2013) and European localities (Gómez et al., 2007; Larsson, 2009; Van De Schootbrugge et al., 2009; Götz et al., 2009; Bonis et al., 2009, 2010; Bonis and Kürschner, 2012) collectively indicate a more muted plant diversity decline than the macrofloras - likely due to coarser taxonomic resolution of pollen and spore studies (Mander et al., 2010). Nevertheless, these palynological analyses support a floristic transitional period in the latest Rhaetian to earliest Hettangian (ca. 201.4 Ma) (Hesselbo et al., 2002; Mander et al., 2013). The majority of analyses demonstrate compelling evidence for biotic responses to extreme environmental perturbance including fern spore spikes (Van De Schootbrugge et al., 2009; Lindström, 2016), declines in diversity (Bonis and Kürschner, 2012), and/or intervals with dark, malformed, or reproductively altered palynomorphs (Visscher et al., 2004; Mander et al., 2012; Kürschner et al., 2013; Lindström et al., 2019; Vajda et al., 2023). In this study, we define the Tr–J 'transition' as a biotic transitional period in response to environmental change characterised by a floristic turnover, linked to CAMP activity via the stable carbon isotopic record.

Stable carbon isotope data show a succession of negative and positive carbon isotope excursions (CIEs) across the Tr–J transition, thought to represent changes in the global exogenic carbon cycle. Release of ^{13}C-depleted CO_2 from volcanic degassing, caused negative $\delta^{13}C$ excursions (anomalies) in the earth system (Kump and Arthur, 1999; Capriolo et al., 2020). Hesselbo et al. (2002) identified an 'initial' negative CIE of ~ −4 ‰ within bulk organic matter ($\delta^{13}C_{org}$) in the Cotham Member at St Audrie's Bay (UK), followed by a second negative 'main' CIE in the Blue Lias Formation; consistent with isotopically light carbon from CAMP CO_2 degassing. These features were also correlated to a negative $\delta^{13}C_{org}$ excursion from the Hettangian stage GSSP (Global Stratotype Section and Point) Kendlbach Formation, Tiefengraben Member (West Kuhjoch, Austria) (Kürschner et al., 2007; Ruhl et al., 2009; Hillebrandt et al., 2013). The 'initial' CIE was also correlated with the most significant anomaly in the Nézsa-Csővár Block (Hungary) (Kovács et al., 2020).

From the Jameson Land succession at Astartekløft, isotopic values from charcoal ($\delta^{13}C_{wood}$) demonstrate a single negative anomaly interpreted as a combination of the 'initial' and 'main' isotope excursions observed in the expanded marine sections at St Audrie's Bay (Hesselbo et al., 2002). The timing of the most negative values of the CIE (~ −3.5 ‰) corresponds to the base of the *Thaumatopteris* zone, at above 45 m level in the section (Harris bed D/Astartekløft bed 5) (Fig. 2). Mander et al. (2013) described four local sporomorph assemblage zones at Astartekløft (Figs. 3 and 8) and correlated this zonation to St Audrie's Bay, suggesting Astartekløft fossiliferous beds 1–4 are correlative with the lower Cotham Member and Astartekløft bed 5 represents the onset of the 'main' negative carbon isotope excursion.

Palaeoecological analysis of the Astartekløft sequence shows a 35 % loss in plant generic diversity before the Tr–J transition zone (McElwain et al., 2007). A similar magnitude generic extirpation is not known in other end-Triassic floristic assemblages and we propose this reflects a lack of palaeoecological investigations based on census collections. The census method samples a complete population of fossil plant morphotaxa preserved in a locality within a standardized volume of rock and sampling time frame (e.g. Kidwell and Flessa, 1998; Johnson, 2002; McElwain et al., 2007; Bercovici et al., 2008; Burnham, 2008; Wing et al., 2012; Contreras, 2018; Allen et al., 2020). Census collected floras enable calculation of the relative abundance of fossil taxa and their palaeoecological role (dominant or rare) (McElwain et al., 2007), rather than just their presence or absence as more commonly reported (e.g. Barbacka et al., 2017). The flora of the nearby South Tancrediakløft locality described by Harris (1937) as presence-absence data, captures the Tr–J transitional period yet the paleoecology remains unstudied. Observing palaeo-diversity and macroecological change based on relative abundance datasets across the Tr–J transition (ca. 201.4 Ma) allows for insights on how plant diversity is affected over time, and on the mechanisms by which environmental stress can drive ecosystem collapse and recovery. Further, our palaeoecological study of South Tancrediakløft permits a regional-scale evaluation of the end-Triassic vegetation and allows for more insight on whether the variation in the interpreted depositional environments influenced floristic composition and Tr–J ecological turnover.

South Tancrediakløft located at 70.47°N, 22.62°W, 16.5 km due south of Astartekløft, outcrops on the western shore of Hurry Inlet (Fig. 1). Here we present original data on the generic plant palaeoecology and palaeodiversity of this locality based on a census of 2369 fossil leaves collected in the summer of 2004. This locality is one of 13 first described by T.M. Harris between 1926 and 1937 (Harris, 1926, 1931, 1932a, 1932b, 1935, 1937) of the Kap Stewart Group. The locality was selected for this study as it shows a greater variation in depositional environments, and possibly taphonomic processes (e.g. biostratinomy and fossil diagenesis) compared to Astartekløft. We use generic relative abundance data to assess plant community composition paired with measures of biodiversity (generic richness and evenness) to determine ecosystem stability across the Triassic–Jurassic boundary interval. The taphonomy was assessed to investigate the relative roles of plant preservation quality and depositional setting on the interpretation of paleovegetation dynamics. Additionally, we report a new stable carbon isotope stratigraphy for South Tancrediakløft and correlate it to St Audrie's Bay, UK (Hesselbo et al., 2002), to provide relative temporal constraints on palaeoecological trends.

2. Geologic, climatic and biotic context

2.1. Geological setting of South Tancrediakløft

The succession exposed at South Tancrediakløft belongs to the top of the Innakajik Formation and the Primulaelv Formation of the Kap Stewart Group at the southern end of the East Greenland rift system (Clemmensen, 1980; Surlyk et al., 1981; Surlyk et al., 1986, 2021). The basin is surrounded by the Kong Oscar Fjord regional fault system on the north side, by the Liverpool Land area on the east, and by a N-S trending fault on the west side (Surlyk, 1990; Surlyk et al., 2021). The southern border land was situated close to the present-day south coast of Jameson Land (Surlyk, unpublished data). The Kap Stewart Group sections studied and sampled at South Tancrediakløft are considered to range from latest Rhaetian to earliest Hettangian in age (ca. 201.4 Ma) and

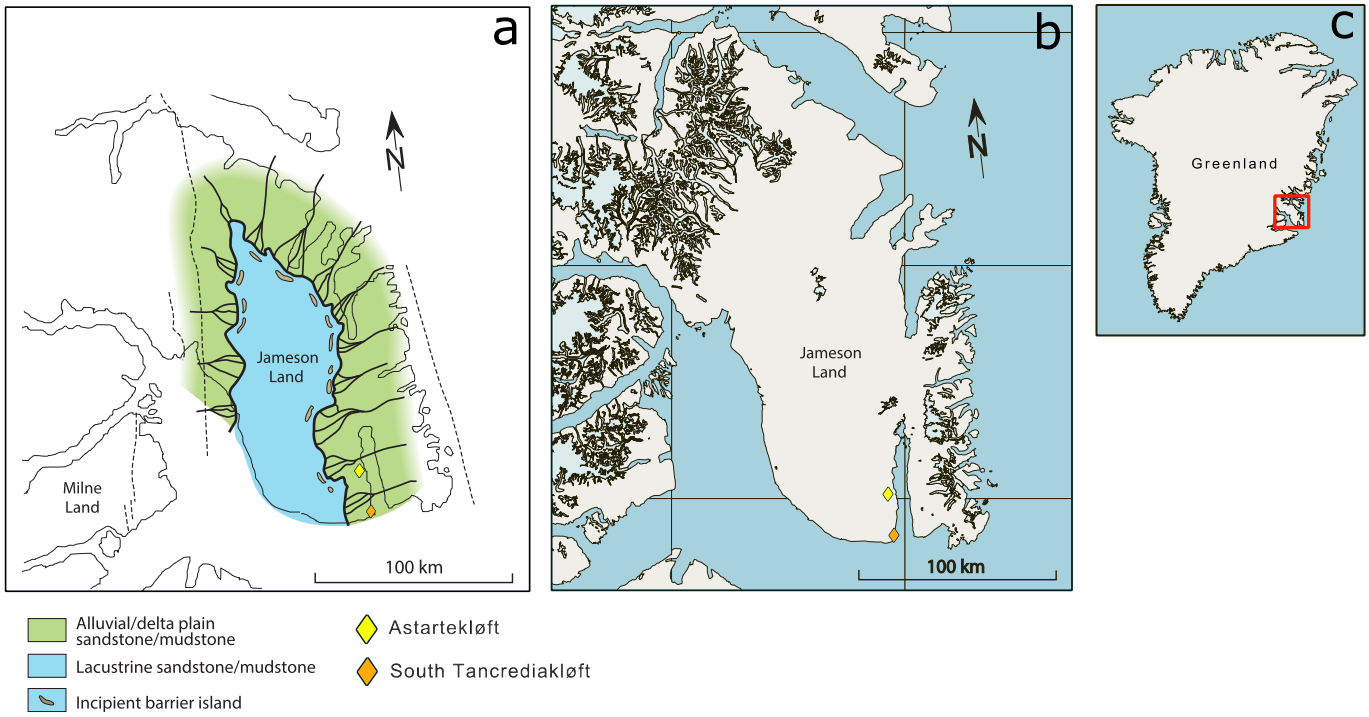

Fig. 1. Maps of the East Greenland, Jameson Land Basin (Kap Stewart Group). Map A shows a palaeogeographic map depicting the Rhaetian-Sinemurian fluvio-lacustrine environment, modified from Surlyk (2003). Map B shows a modern equivalent of map A. Map C shows the current continental position of Jameson Land. The map key indicates the types of depositional environments and the diamonds correspond to the localities South Tancrediakløft (orange) and Astartekløft (yellow). (For interpretation of the references to colour in this figure legend, the reader is referred to the web version of this article.)

contain seven fossiliferous beds (Bed 1, 2a, 2b, 2c, 3, 3b, and 4; see Fig. 2). The South Tancrediakløft succession is about 105 m thick and consists of fine-grain to pebbly sandstones, black/dark grey mudstones, and thin coal beds, deposited in a fluvial-lacustrine setting. The succession is also abundant in plant organs, rootlets, spores and pollen (Dam and Surlyk, 1993; Surlyk et al., 2021). The plant-bearing beds are predominantly dark-grey mudstone 2–5 m thick. These mudstone beds alternate with fine-grained to pebbly sandstones (Fig. 2). Variation in lithology across the Jameson Land Basin is described in Surlyk et al. (2021). The Kap Stewart Group includes two well-described plant macrofossil biozones used by Harris (1937) to define the Tr–J transition; one characterised by the presence of the seed fern *Lepidopteris ottonis* (Rhaetian range zone) and the other by the presence of the fern *Thaumatopteris brauniana* and the absence of L. *ottonis* (Hettangian–Sinemurian range zone). South Tancrediakløft bed 3b shares a similar lithology to the 'Neill Klinter Coal' section of Harris (1937) and to Astartekløft bed 6 (McElwain et al., 2007) (Fig. 2).

2.2. Palaeoclimate setting of South Tancrediakløft

Proxy-CO_2 estimates spanning the Tr–J transition indicate an atmospheric CO_2 doubling to tripling from 990 to 1600 ppm for the latest Rhaetian to 1481–3018 ppm for the earliest Hettangian (McElwain and Steinthorsdottir, 2017). The elevated greenhouse effect on climate caused significant global warming of 3–4 °C globally (McElwain et al., 1999; Steinthorsdottir et al., 2011), increased humidity throughout regions of the Pangaean supercontinent (Bonis et al., 2010) and Milankovitch-type climatic perturbations suggesting monsoonal periods (Ruhl et al., 2010; Bonis and Kürschner, 2012). The lower-mid latitudes, such as the coastal areas of in the northern Tethyan realm (i.e. East Greenland) were likely influenced by oceanic humidity via atmospheric moisture fluctuations. This would have created seasonally wetter conditions, giving rise to a rich vegetation, as represented by the abundant plant fossil record from the area (Rees et al., 2000; McElwain et al., 2007; Van De Schootbrugge et al., 2009; Bonis et al., 2009; Bonis et al., 2010). Floristic records from the eastern Tethyan realm (present-day China) suggest diverse coastal vegetation cover (Li et al., 2020).

During the Late Triassic, the Jameson Land Basin was situated at ca. 35°N in the interior of Laurasia (Kent and Clemmensen, 1996). Climate models for the end-Rhaetian Jameson Land Basin suggest dry climates with annual precipitation under 700 mm/yr, low soil moisture levels in the summer, and a maximum soil moisture of 40 mm in winter (Kutzbach, 1994). Temperatures for the Basin ranged from ca. 10 °C in the winter to 45 °C in the summer. Models including orbital change and climatic extremes show increased seasonality in the northern hemisphere and monsoonal circulation (leading to ±25 % increase in summer precipitation). The deposition of sandstones present in the Jameson Land Basin have therefore been associated with the progradation of storm-dominated deltas and the formation of crevasse splays from monsoonal flood episodes (Dam and Surlyk, 1993).

2.3. Taphonomic context

Taphonomy may be subdivided into necrobiosis (biological and environmental processes), biostratinomy (transportation, decay, and deposition), and fossil diagenesis (all chemical, physical, and biological processes occurring after burial) (Martín-Closas and Gomez, 2004). Viewing palaeoecology as being taphonomically 'filtered' is essential in understanding potential biases. Fossil plant assemblages are automatically biased before collection, and may be further biased by collection unless census protocols are followed. These biases often lead to an over- or underestimation of local communities (Spicer and Greer, 1986; Behrensmeyer et al., 2000). The depositional environments of fossil plant-bearing beds at South Tancrediakløft encompass an array of fluvial-lacustrine environments (Table 1). They differ from those described at Astartekløft, which are isotaphonomic and are interpreted as abandoned channels and sheet splays deposited in alluvial plain environments, containing predominantly parautochthonous fossil plants

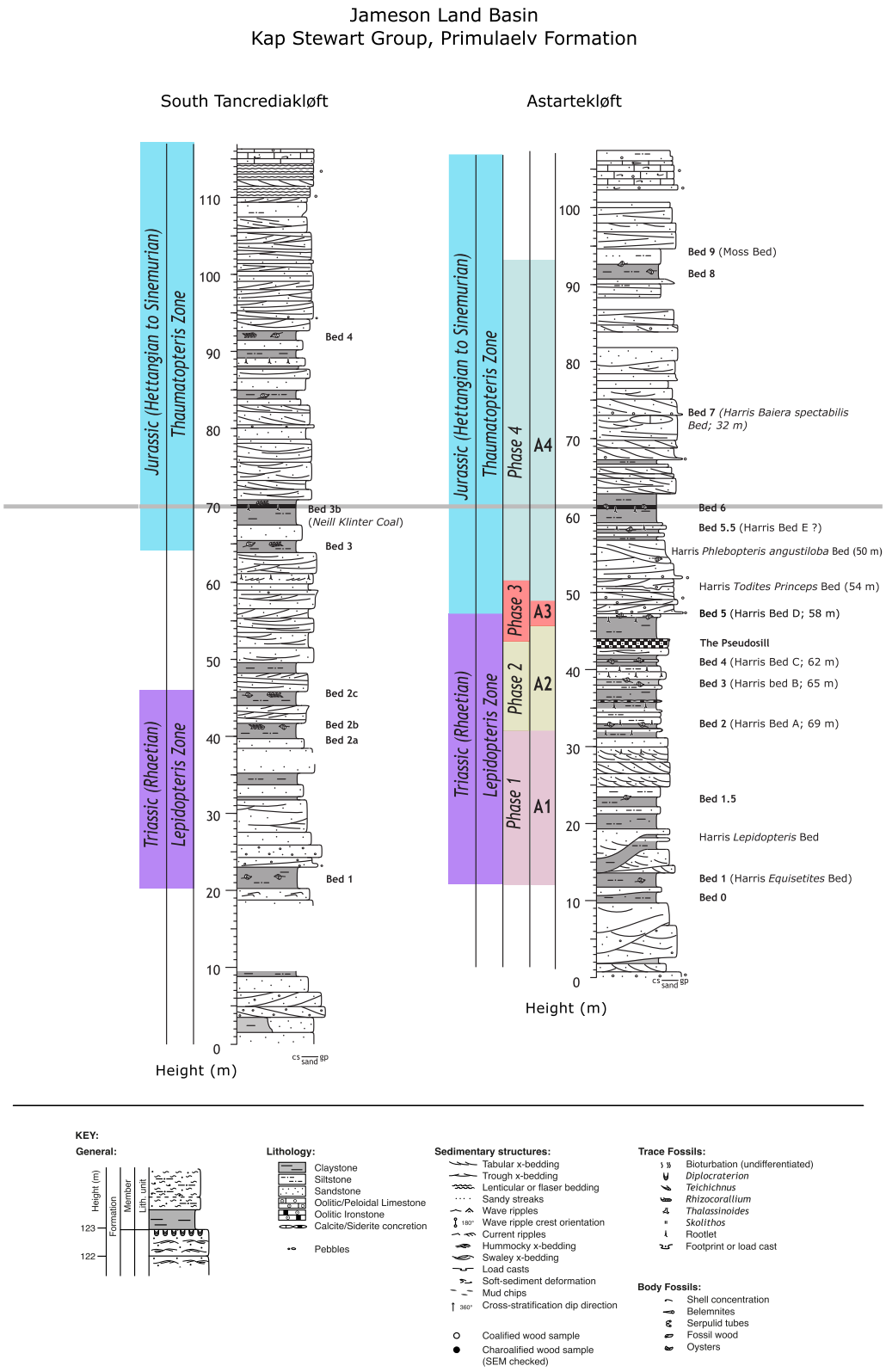

Fig. 2. Stratigraphic log of Jameson Land localities Astartekløft and South Tancrediakløft showing the Harris biozones and beds (Harris, 1937). The beds at Astartekløft were interpreted as follows by McElwain et al. (2007): beds 1–4 belong to the Rhaetian *Lepidopteris* biozone of Harris (1937) (purple). Bed 5 corresponds to plant bed D of Harris (1937) and is described as the Tr–J Transitional bed. Beds 6–8 belong to the Hettangian *Thaumatopteris* biozone (blue). Bed 6 contains charcoal/coal (shares a similar lithology to South Tancrediakløft bed 3b; Harris's *Neill Klinter Coal*). Beds 0, 5.5, and 9 (moss bed) were not investigated in McElwain et al. (2007) and are therefore not addressed in this study. The scale included in these logs indicates height upwards from the base of the succession. For Astartekløft, the ecological phases (Phase 1–4) from McElwain et al. (2007) are also shown alongside the sporomorph assemblage zones (A1-A4) from Mander et al. (2013). (For interpretation of the references to colour in this figure legend, the reader is referred to the web version of this article.)

Table 1
Depiction of the fossiliferous beds at South Tancrediakløft with their corresponding geologic age, depositional environment, taphonomy, number of hand specimens recorded (rock slabs), and number of leaf macrofossils recorded.

Harris (1937) macrofloristic biozonation	Bed	Age	Depositional environment	Taphonomy
Thaumatopteris	4	Hettangian (Jurassic)	Lake	Parautochthonous
Thaumatopteris	3b	Hettangian (Jurassic)	Swamp	Parautochthonous
Thaumatopteris 1st occurrence	3	Hettangian (Jurassic)	Lake	Parautochthonous
Lepidopteris	2c	Rhaetian (Triassic)	Abandoned crevasse splay	Parautochthonous
Lepidopteris	2b	Rhaetian (Triassic)	Crevasse splay	Parautochthonous
Lepidopteris	2a	Rhaetian (Triassic)	Storm-influenced lake margin	Parautochthonous
Lepidopteris	1	Rhaetian (Triassic)	Lake	Parautochthonous

(McElwain et al., 2007).

3. Material and methods

3.1. Census collection and curation of South Tancrediakløft plant fossils

The assemblages of compression/carbonisation plant macrofossils were excavated in 2004. The assemblage was collected following a census method (McElwain et al., 2007; Burnham, 2008; Contreras, 2018, and references therein) to avoid collector bias and to reconstruct the dominance and diversity patterns of the fossil plant assemblages. Each bed was sampled horizontally as widely as the exposure would allow, this reduced biases due to localised over-representation of taxa. These fossils are currently housed at the Trinity College Dublin Geological Museum (field specimen numbers 50,051 to 51,752 – originally designated as palaeobotanical Field Museum of Natural History collections numbers). Hand specimens were recorded and examined for leaf fossils following standard protocols (Popa, 2011; Cleal et al., 2021; Pardoe et al., 2021) (i.e. Table 2 in section 4.2). Every fragmentary or whole leaf fossil with sufficient identifiable characters was identified to fossil morphogenus or to morphospecies if very distinguishable using morphological keys (Popa and McElwain, 2009), and reference to the Harris monographs (Harris, 1926, 1931, 1932a, 1932b, 1935, 1937). Microscopy has not been undertaken to further classify each morphotype to morphospecies, hence morphospecies identifications are still preliminary. Specimens that could not be identified without microscopy and/or specimens classified as 'debris' are not included in these data, and amount to <2 % of the flora per bed. Each identified leaf fossil was taphonomically graded for preservation, transport, presence/absence of cuticle, and the presence/absence of coalified tissue. Fossil morphotaxa were quantified to determine relative abundance following McElwain et al. (2007). Briefly, per hand sample (rock slab), each fossil plant morphotype/morphogenus was recorded separately, and up to a maximum of five occurrences were counted (see Supplementary Materials). This method differentiates individual macrofossils on hand samples (Popa, 2011).

3.2. Method for stable carbon isotope stratigraphy of South Tancrediakløft

A stable carbon isotope stratigraphy based on fossil wood was developed for South Tancrediakløft. Meso- and macro-fossil wood preserved in mostly coalified form (with a few charcoalified) was sampled in the field with stratigraphic positions accurately recorded. And processed following standard protocols (see Supplementary Materials).

3.3. Palaeoecology and palaeodiversity analyses of South Tancrediakløft

All palaeoecological and palaeodiversity analyses are based only on vegetative plant macrofossil parts (leaves) classified to morphogenus and are presented in abundance (Table 2 in section 4.2). A test of distortion effects on the palaeoecological and palaeodiversity analyses was undertaken by including and excluding the South Tancrediakløft bed with the least occurrences (bed 2a). However, our rarefaction analysis still contains bed 2a as it did not significantly skew the data. A relative abundance matrix of morphogenera was created from the raw abundance of all fossil leaves per fossiliferous bed. Percentages of fossil morphotaxa per bed were also calculated to assess ecological dominance and the rank order of morphotaxa. Floristic turnover is quantified by change in community composition and change in total abundance of an assemblage (Anderson et al., 2011; Shimadzu et al., 2015).

The relative abundance of morphogenera was used alongside measures of biodiversity to determine dominant morphotaxa within the ecosystem, and to identify rare morphogenera per fossiliferous bed throughout the section. In this study, palaeodiversity was determined via measures of generic richness (number of morphotaxa) and evenness (similarity of abundances of morphotaxa within an environment) (Shannon's Diversity Index; $H = -\Sigma_i \frac{n_i}{n} ln \frac{n_i}{n}$) (Hammer et al., 2001). Relative abundance percentages were calculated for dominant floristic groups per bed to assess response to environmental disturbances. For all 7 fossiliferous beds, absolute generic richness was standardized using rarefaction analysis with 95 % confidence intervals via *Analytic Rarefaction 1.3* (Holland, 2003). Rarefaction is ideal for fossil plant richness estimates as it is robust against incomplete or varied datasets. Rarefaction curves were constructed to evaluate whether sampling was sufficiently intense to be representative of the temporal variations in standing vegetation, as preserved in the fossiliferous beds. A rarefaction curve that has plateaued at or below the actual sampling intensity indicates a sufficient sampling intensity, i.e. the rarefied curve is representative of the tested community's richness.

Total biodiversity loss was estimated simply by deducting the average of the total rarefied value per bed from the preceding beds (e.g. if bed 1 = 12; bed 2b = 10; bed 2c = 6. The average of beds 1 and 2b is 11. (6/11) * 100 = ~ 54 %). The same method was used to determine recovery flora and was replicated from McElwain et al. (2007). This method quantifies occurrences in all beds preceding the measured bed to ensure no occurrences are excluded. This is of importance as patterns in floristic turnover or extirpation could be missed, giving a false interpretation of biodiversity patterns through time.

3.4. Taphonomic influences on interpretations of palaeoecology and palaeodiversity

The relative influence of plant taphonomy on the interpretation of palaeoecology and palaeodiversity was assessed using multivariate statistical analyses, rarefaction, and linear regression. Firstly, transport and preservation quality were assessed for each hand specimen (Table 2 and Table A in Supplementary Materials). We assessed damage for each hand specimen, separately considering leaf fragmentation and tissue abrasion. It is generally inferred that greater damage to leaf fossils is associated with long-distance transport, high-energy waterflow and/or lengthy exposure in the water column (Spicer, 1981). Fossil plant preservation was classified as 'poor', 'good' or 'excellent' based on the degree of leaf damage noted, and transport was classified as 'local', 'riparian' or 'distant' (i.e., autochthonous, parautochthonous, or allochthonous) based on the average of all macrofossil leaf fragmentation observed per hand specimen (Table 1). Although autochthonous assemblages are optimal, parautochthonous assemblages offer a census of riparian and local vegetation. Allochthonous assemblages are not

applicable to South Tancrediakløft. Complexities such as mixocoenoses (i.e. Barrón and Comas-Rengifo, 2007) are not accounted for in this study. All results on the taphonomic influences on interpretations of palaeoecology and palaeodiversity can be found in the Supplementary Materials.

3.5. Comparison of South Tancrediakløft and Astartekløft

The successions at South Tancrediakløft, Astartekløft, and the initial collections described by Harris (1937) were compared and correlated using the Harris macrofossil biozones. Additionally, a new $\delta^{13}C_{wood}$ record from charcoal of South Tancrediakløft was used to chemostratigraphically correlate the $\delta^{13}C_{wood}$ record of Astartekløft and St Audrie's Bay (UK) (Hesselbo et al., 2002; Mander et al., 2013). To explore multivariate relationships in fossil plant community data within and between the two successions, NMDS was used (PAST 4; Hammer et al., 2001).This multivariate exploratory ordination technique was selected as it is effective for expressing community gradients and is commonly

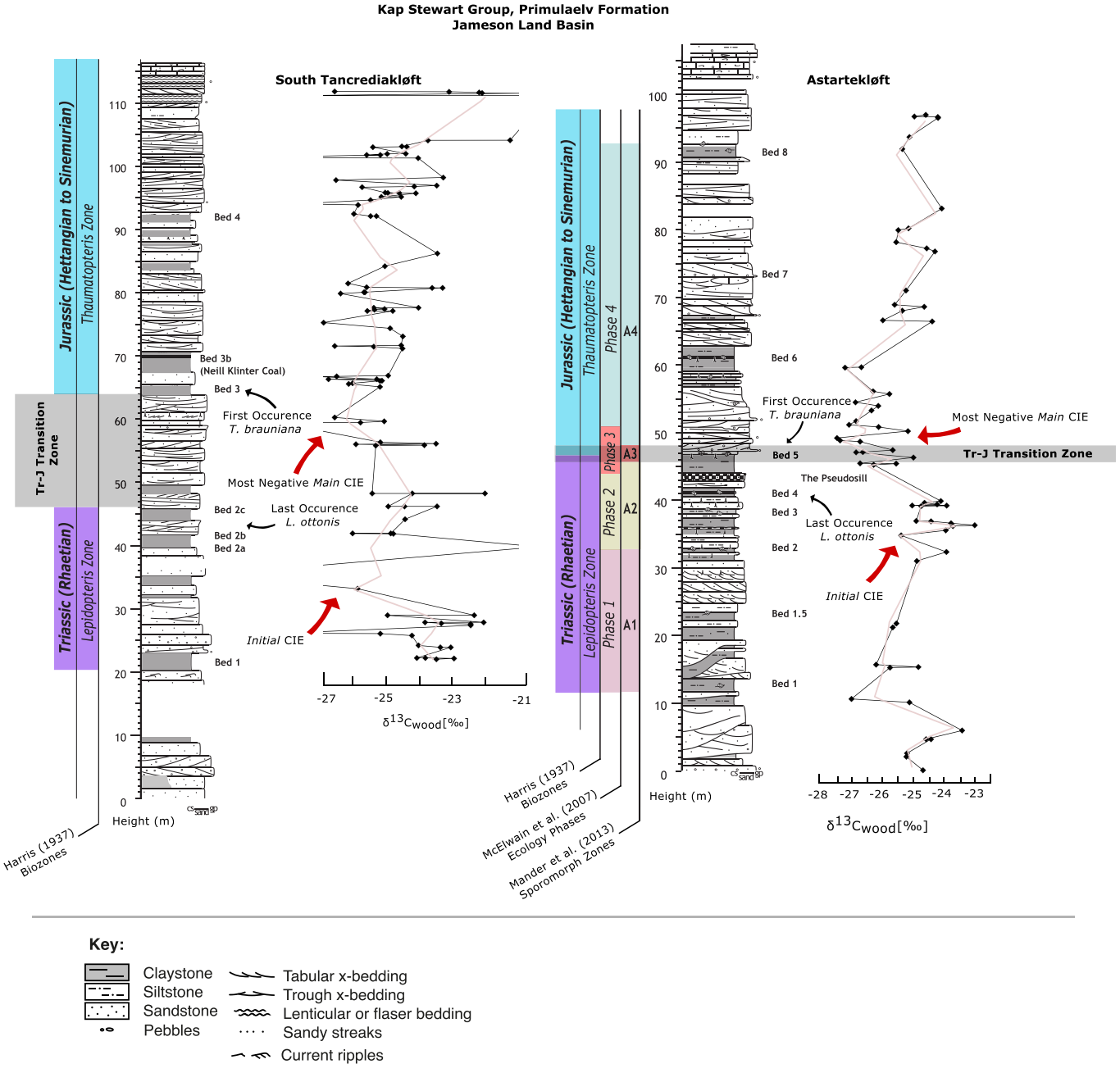

Fig. 3. Stable carbon isotope stratigraphy for South Tancrediakløft based on $\delta^{13}C_{wood}$ measurements from raw fossilised and charcoalified wood fragments collected in the field by S.P. Hesselbo in 2004; positioned next to the stable carbon isotope stratigraphy for Astartekløft (also $\delta^{13}C_{wood}$ measurements from raw fossilised and charcoalified wood fragments) from Hesselbo et al. (2002). Both South Tancrediakløft and Astartekløft logs show biozonation from Harris (1937) and division of the section into Triassic Rhaetian (purple), transition zone (grey) and Jurassic Hettangian (blue) as well as the last and first occurrence of biozone indicator taxa *Lepidopteris ottonis* and *Thaumatopteris brauniana*. Astartekløft also shows zonation from McElwain et al. (2007) (ecology zones 1–4) and Mander et al. (2013) (sporomorph assemblage zones 1–4). For the stable carbon isotope stratigraphy, a LOESS curve with 0.10 fitting parameter (pink) has been plotted through the raw to identify major trends in the data. The anomalies associated with St Audrie's Bay 'initial' and 'main' negative excursions (Hesselbo et al., 2002) are indicated by the red arrows. (For interpretation of the references to colour in this figure legend, the reader is referred to the web version of this article.)

used in palaeoecology (e.g. Pryor and Gastaldo, 2000; Barral et al., 2016). The Bray-Curtis similarity index was used for the NMDS, as it takes abundance into account unlike other methods based on presence/absence (Bray and Curtis, 1957). Fossiliferous beds sharing greater similarity across all generic abundances cluster together in NMDS space, which orientates the samples along the NMDS axes by their distribution of generic abundances. The significance of multivariate differences was tested using Permutation Analysis of Variance (PERMANOVA) (PAST 4; Hammer et al., 2001).

4. Results

4.1. New isotope stratigraphy

An average ~ −3 ‰ negative CIE is identified by LOESS regression at 34.9 m in the South Tancrediakløft section within the *Lepidopteris* zone. An average ~ −2 ‰ excursion occurs at 58.5 m within the Tr–J transition zone (Fig. 3). Considering the raw data and not excluding outliers or averaging the data with LOESS, the total negative excursion at 34.9 m exceeds 8 ‰ and the negative excursion at 58.5 is >5 ‰. Based on lithostratigraphic and floristic correlations with Astartekløft (Fig. 2, Tables 1 and 2), we interpret the negative excursion in the lowest part of the section of South Tancrediakløft as representing the 'initial' global CIE at Saint Audrie's Bay (Hesselbo et al., 2002), and the excursion within the transition zone as representing the 'main' global CIE. Stable carbon isotopic composition returns to background values after the 'initial' and prior to the 'main' isotope excursion at South Tancrediakløft. A > 4 ‰ positive CIE occurs at 102.3 m at South Tancrediakløft which likely correlates with similar magnitude excursions at Astartekløft at 84.8 m and at St Audrie's Bay at 24.1 m.

In Mander et al. (2013), the stratigraphic position of Astartekløft plant bed 5 corresponds to the first occurrence of the sporomorph *Cerebropollenites thiergartii* and the onset of the 'main' negative CIE in the St Audrie's Bay Pre-Planorbis bed at ~17.5 m (Hesselbo et al., 2002). Consequently, the negative CIE recorded at Astartekløft (~ 48.7 m) correlates to the onset of 'main' negative CIE and the position of the 'initial' excursion should lie somewhere between macrofossil beds 4 and 5. Considering how well the fossil plant bed ecology and diversity metrics align for Astartekløft and South Tancrediakløft, it is more likely that the sharp negative excursion around bed 3 (~ 34.3 m) at Astartekløft marks the position of the initial CIE. This sharp negative CIE at ~34.3 m correlates to the initial excursion at South Tancrediakløft at 34.9 m (Fig. 3).

4.2. Palaeoecology analysis

A total of 2369 leaf macrofossil were identified to 27 unique morphogenera, associated with ferns, bennettites, cycads, ginkgoes, and conifers (Table 2). The complete dataset is available via the provided link. The floristic composition varies notably across fossiliferous beds and shows that no single plant group is dominant through the entirety of the studied succession. The peltasperm *Lepidopteris* occurs at South Tancrediakløft until the uppermost Triassic (bed 2c), consistent with Astartekløft and the *Lepidopteris* zone. Together, *Lepidopteris*, *Ptilozamites* (pteridosperm; Popa and McElwain, 2009), and *Pterophyllum* (bennettite) comprise 76 % of the lowermost end-Rhaetian bed (bed 1) at South Tancrediakløft. In this assemblage, *Pterophyllum* and *Anomozamites* are representative of the bennettites and commonly occur until bed 3 (Table 2), the closest stratigraphically to Astartekløft bed 5.

A floristic shift in dominance occurs at South Tancrediakløft in the lowest Jurassic beds (3, 3b, and 4) with the rise of conifer and ginkgo trees. Notable abundances of these morphotaxa are 43 % *Podozamites* in bed 3; 64 % *Czekanowskia* and 32 % *Ginkgoites* in bed 3b; 46 % *Baiera*, 31 % *Podozamites* and 16 % *Sphenobaiera* in bed 4 (Table 2). Cumulatively, ginkgo abundance increases in the lowermost Jurassic beds (total percentage of ginkgoes per bed) from 0.7 % in bed 3, 32 % in bed 3b, to 64 % in bed 4.

The Triassic beds (bed 1-2c) contain 42.4 % lower-canopy morphotaxa, 35.7 % mid-canopy morphotaxa, and 21.9 % upper-canopy morphotaxa. The Jurassic beds (3–4) contain 5.31 % lower canopy morphotaxa, 12.7 % mid-canopy morphotaxa, and 82 % upper-canopy morphotaxa. The upper-canopy is characterised by ginkgoes and

Table 2
Generic abundance table showing number of vegetative occurrences (macrofossil leaves) per bed at South Tancrediakløft. Percentage representation of generic abundance is shown in parentheses. Totals of hand samples and macrofossil leaves per bed are shown below.

Macrofossil Taxon	Bed 1	Bed 2a	Bed 2b	Bed 2c	Bed 3	Bed 3b	Bed 4
Anomozamites	71 (10.8)	0	25 (11.8)	2 (6.9)	1 (0.17)	0	0
Baiera	0	0	0	0	1 (0.17)	0	336 (47.9)
Cladophlebis	0	0	0	0	10 (1.72)	0	0
Ctenis	1 (0.15)	0	0	0	0	0	0
Czekanowskia	0	0	0	0	31 (5.34)	125 (65.1)	0
Dictyophyllum	1 (0.15)	0	61 (28.9)	2 (6.9)	46 (7.93)	0	8 (1.14)
Drepanozamites	5 (0.77)	0	0	0	0	0	0
Elatocladus	8 (1.23)	0	1 (0.47)	0	2 (0.34)	0	0
Equisetites	4 (0.61)	0	84 (39.8)	12 (41.4)	3 (0.52)	0	16 (2.28)
Ginkgoites	0	0	0	0	3 (0.52)	62 (32.3)	6 (0.85)
Lepidopteris	175 (26.8)	3 (75)	31 (14.7)	1 (3.45)	0	0	0
Marattia	1 (0.15)	0	0	0	29 (5)	0	0
Marattiopsis	1 (0.15)	0	0	0	0	0	0
Neocalamites	0	0	2 (0.95)	1 (3.45)	0	0	1 (0.14)
Nilssonia	5 (0.77)	0	0	0	64 (11.3)	0	2 (0.3)
Ontheodendron	0	0	0	0	2 (0.34)	0	0
Osmundopsis	0	0	0	0	7 (1.21)	0	0
Podozamites	5 (0.77)	0	1 (0.48)	0	254 (43.8)	5 (2.6)	217 (30.9)
Pterophyllum	163 (25)	1 (25)	3 (1.42)	11 (37.9)	118 (20.3)	0	0
Ptilophyllum	25 (3.83)	0	0	0	0	0	0
Ptilozamites	159 (24.3)	0	2 (0.95)	0	0	0	0
Sphenobaiera	0	0	0	0	0	0	115 (16.4)
Stachyotaxus	21 (3.22)	0	0	0	1 (0.17)	0	0
Taeniopteris	5 (0.77)	0	1 (0.47)	0	0	0	0
Thaumatopteris	0	0	0	0	6 (1.03)	0	0
Todites	0	0	0	0	2 (0.34)	0	0
Weilandiella	2 (0.31)	0	0	0	0	0	0
Total Macrofossil Leaves	652	4	211	29	580	192	701
Total Hand Samples	286	2	86	20	202	28	113

conifers, the mid-canopy by bennettites and cycads, and the lower by ferns and lianas. A notable loss is seen in both the lower and mid-canopy in the Jurassic with a 37 % and 23 % decline respectively. The few occurrences for these mid- and lower-canopy morphotaxa in the Jurassic are *Nilssonia*, *Neocalamites*, *Equisetites*, and *Dictyophyllum*. Fern morphotaxa are notably abundant at beds 2b (68 %) and 2c (48 %). The morphogenera included in this sum are *Cladophlebis*, *Dictyophyllum*, *Marattia*, *Osmundopsis*, *Todites*, and *Equisetites* (e.g. fern-spikes; Thomas and Cleal, 2022).

4.3. Palaeodiversity analysis

A ~ 54 % loss in generic richness is observed in South Tancrediakløft before bed 3 (from bed 1- 2c), indicating a profound plant biodiversity loss in the latest Triassic (Fig. 4). No clear differences are observed in generic level floristic richness when summed per period (Rhaetian vs Hettangian) for either locality. Substantial fluctuations in fossil plant generic richness are, however, observed through time at South Tancrediakløft with greater richness in beds 1, 3, and 4. Lower richness was observed in beds 2b, 2c, and 3b. Our results show a plateaued curve for bed 3b, indicating the total rarefied leaf morphogenera is representative of the tested community richness, regardless of the composition being characterised by only three morphotaxa. Whereas, the curves for beds 2b, 2c, and 3 do not reach a plateau in our analysis thus indicating an insufficient sampling intensity. Although, here diversity is estimated from generic richness and community evenness, Figs. 6 and 7 containing Shannon Index (H) results for both localities are shown in Section 4.4 to facilitate comparisons.

4.4. Comparison of South Tancrediakløft and Astartekløft

The census collected section at Astartekløft recovered more leaf macrofossils and more unique morphogenera across more fossiliferous beds than in South Tancrediakløft. At Astartekløft, the Tr–J transition (Bed 5) is characterised by mixed assemblages of both latest Triassic and earliest Jurassic macrofloristic elements. This transition is not captured in any of the fossil plant beds collected from South Tancrediakløft. Sporomorph zonation (Zone A3) with the earliest occurrence of *Cerebropollenites thiergartii* in Astartekløft bed 5 correlates approximately to the onset of the 'main' carbon isotopic excursion in the marine upper pre-Planorbis beds of St Audrie's Bay (Mander et al., 2013). Based on the detailed logs (Fig. 2) and isotope-stratigraphy (see Sections 4.1 and 5), we infer that equivalent strata to the transition zone (bed 5) at Astartekløft lie somewhere between South Tancrediakløft beds 2c and 3, at around 56 m in the section and within a fossiliferous sandstone.

The floristic composition in South Tancrediakløft, relative to Astartekløft (cf. McElwain et al., 2007, abundance matrix) is largely similar and driven by the occurrences of bennettites *Pterophyllum* and *Anomozamites*, cycad *Nilssonia*, and fern *Thaumatopteris*. There is a clear distinction between the Rhaetian and Hettangian biozones seen in South Tancrediakløft beds 2c and 3, with the last occurrence of L. *ottonis* in bed 2c and the first occurrence of *T. brauniana* in bed 3 (see Table 2). Therefore, bed 3 is clearly marked as a Jurassic bed, not as a Tr–J transition bed. This is supported by the observation that no plant bed at South Tancrediakløft sufficiently matches the composition of Astartekløft bed 5. However, bed 3 is the only Jurassic bed at South Tancrediakløft sharing dominant Rhaetian bed 1-like morphotaxa i.e. *Pterophyllum* (Table 2); making its composition a 'mixed-bag', neither like Jurassic beds 3b and 4, nor like Astartekløft bed 5.

To further compare the localities by their floristic composition, NMDS (Non-Metric Dimensional Scaling) ordination analysis was used. NMDS analysis is a powerful statistical technique that allows for the visualization of complex multivariate data by reducing dimensions. In lower-dimensional space, patterns and group structures that may not be apparent in higher dimensions are observable. This method focuses on rank order rather than exact distances, making it robust to non-linear relationships and suitable for ecology data. In Fig. 5, a clear separation between the Triassic beds (purple) and the Jurassic beds (blue) of the two localities is shown. The Astartekløft Tr–J transitional bed (Bed 5) closely aligns with South Tancrediakløft (Bed 3) on coordinate 1. The outliers visible in this plot are Astartekløft bed 3 and bed 6, a Triassic and Jurassic bed respectively. This skew is caused by the absence of the taxon *Baiera* in bed 6 which is a clear grouping criterion for all Jurassic beds (i.e. all other Jurassic beds in both assemblages contain *Baiera*). In addition, *Baiera* is considered as the most abundant ginkgo in both assemblages, though Astartekløft bed 6 contains no ginkgophytes. The stress value for this plot is 0.185. As it is <0.20, the ordination may be misleading for interpretation of minute details. To test these results, the two-way PERMANOVA test (Anderson, 2001) with Bray-Curtis similarity index reported a significant *p*-value of 0.005 for composition

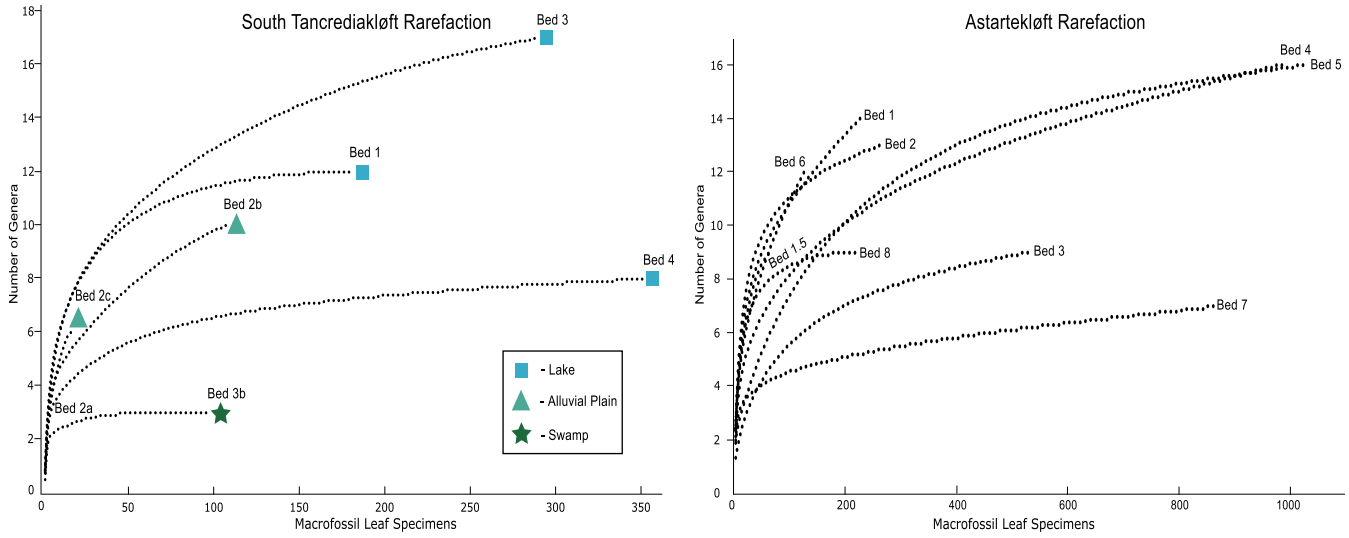

Fig. 4. Rarefied leaf morphogenera per bed estimated via rarefaction analysis for South Tancrediakløft (left) and for Astartekløft (right), plotted by number of morphogenera on the y-axis and macrofossil leaf specimens on the x-axis. No depositional environments are shown for Astartekløft (right) as all beds are interpreted as alluvial plain environments except bed 6 (coal swamp). The beds for both localities are not coloured by period (Triassic vs. Jurassic) as no significant pattern was observed.

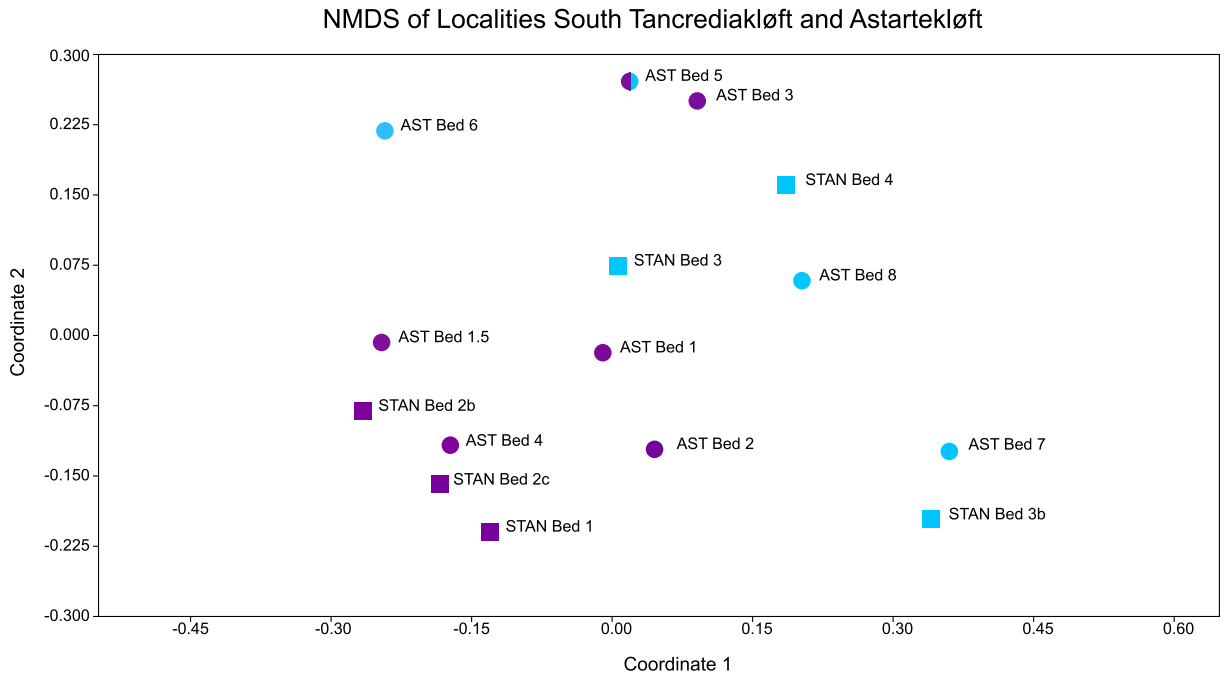

Fig. 5. Non-metric multidimensional scaling (NMDS) ordination scatter plot of localities South Tancrediakløft (squares) and Astartekløft (circles), beds plotted with relative abundance data (macrofossil leaf morphogenera). Beds are temporally grouped into Triassic (purple) and Jurassic (blue). The established Tr–J transition zones are demarked by half blue and half purple for 'AST Bed 5'. Stress value = 0.185. (For interpretation of the references to colour in this figure legend, the reader is referred to the web version of this article.)

groupings by period (Triassic vs Jurassic) and insignificant *p*-values of 0.72 for groupings by locality (South Tancrediakløft vs Astartekløft). In other words, statistical analyses of floristic composition data from both localities reveal a strong regional pattern of floristic change from the late Triassic to the Early Jurassic.

To better visualise trends in evenness for both localities, axis 2 of the NMDS analysis (from Fig. 5) and the $\delta^{13}C$ values (from Fig. 3) are included in Figs. 6 and 7. Axis 2 is clearly representative of the palaeoecology trends of both localities as it shows compositional similarities of the beds. Details on the grouping variable taxa can be found in Table B (Supplementary Materials). South Tancrediakløft shows little variation in evenness values for all beds except bed 2c and 3b, where peak evenness values are evident (Fig. 6). These peaks coincide with the observed fern-spike and coal bed, respectively and they both display a drop in richness (Table 2, Fig. 4). Bed 2a was omitted from this analysis as it is biased by only containing 2 specimens and presenting an extremely high evenness value of 0.99. Evenness trends at Astartekløft (Fig. 7) are more varied through time than at South Tancrediakløft; with an increase in evenness for beds 1, 1.5, 2, and 8, and a decrease in evenness only noted from beds 3–5. The evenness values for South Tancrediakløft (Fig. 6) share a remarkably similar pattern with NMDS axis 2; the beds with higher evenness values (bed 2c and 3b) also have distinct ecological change (higher fern abundance in 2c and homogenised flora in 3b). This mirrored pattern between evenness and NMDS axis 2 is not evident at Astartekløft (Fig. 7).

In Astartekløft axis 2, a sharp direct response to the initial CIE is seen at bed 3 followed by an increase in occurrences for the fern taxon *Dictyophyllum* (key disturbance indicator at South Tancrediakløft) in bed 4 and subsequently followed by the main CIE (bed 5) with a second response which shifts to the negative portion of the axis, returning to the positive half at bed 8. While less pronounced at South Tancrediakløft, the same trend is visible: a response to the initial CIE in beds 2b and 2c (fern spike) followed by the main CIE and a response which shifts to the negative side of the axis (first homogenised flora), then returning to positive values in bed 4.

5. Discussion

Integration of the new stable carbon isotope stratigraphy and results from our census collection for South Tancrediakløft provide a global context for the floristic changes spanning the ETME of East Greenland. In the following sections, we first discuss Astartekløft in the light of this new isotope data, and the major floristic patterns seen within the Jameson Land Basin. Based on this new and reinterpreted isotope stratigraphy, there are nearly >25 m of sediment between the 'initial' and 'main' carbon isotope excursions at Astartekløft and South Tancrediakløft. In contrast, for the (mostly) marine sections of St Audrie's Bay and Kuhjoch (Austria) (Ruhl et al., 2009) there are about 5 and < 4 m of rock respectively between the 'initial' and the 'main' carbon isotope excursions. The terrestrial Upper Triassic–Lower Jurassic sections of Astartekløft and South Tancrediakløft therefore offer unique windows to investigate relatively expanded stratigraphic sections at the critical time interval of the ETME. Four fossiliferous beds occur at or between the 'initial' and 'main' carbon isotope excursions at Astartekløft and three occur bracketed between the same time interval at South Tancrediakløft.

5.1. Floristic turnover prior to Tr–J transition

The fossil flora of South Tancrediakløft demonstrates a strong 54 % loss in generic richness in the uppermost Triassic before the Tr–J transition (beds 2b and 2c). This is evident by the loss of morphotaxa such as bennettites *Anomozamites* and *Ptilophyllum*, the peltasperm *Lepidopteris*, and the pteridosperm *Ptilozamites*, as well as conifers *Stachyotaxus* and *Elatocladus* (Table 2). Compared to Astartekløft, an overall higher fossil floristic diversity is observed for South Tancrediakløft regardless of the smaller sample size (South Tancrediakløft $N = 2369$; Astartekløft $N = 4303$). This greater floristic diversity is clearly evident when observing the data per bed rather than per entire assemblage. Like South Tancrediakløft, Astartekløft shows no division of beds in the rarefaction analysis by period (Fig. 4). A ~ 35 % loss in generic richness was found before (in beds 3 and 4) the Astartekløft Tr–J transition (Bed 5) (McElwain et al., 2007). For South Tancrediakløft, the bed determined

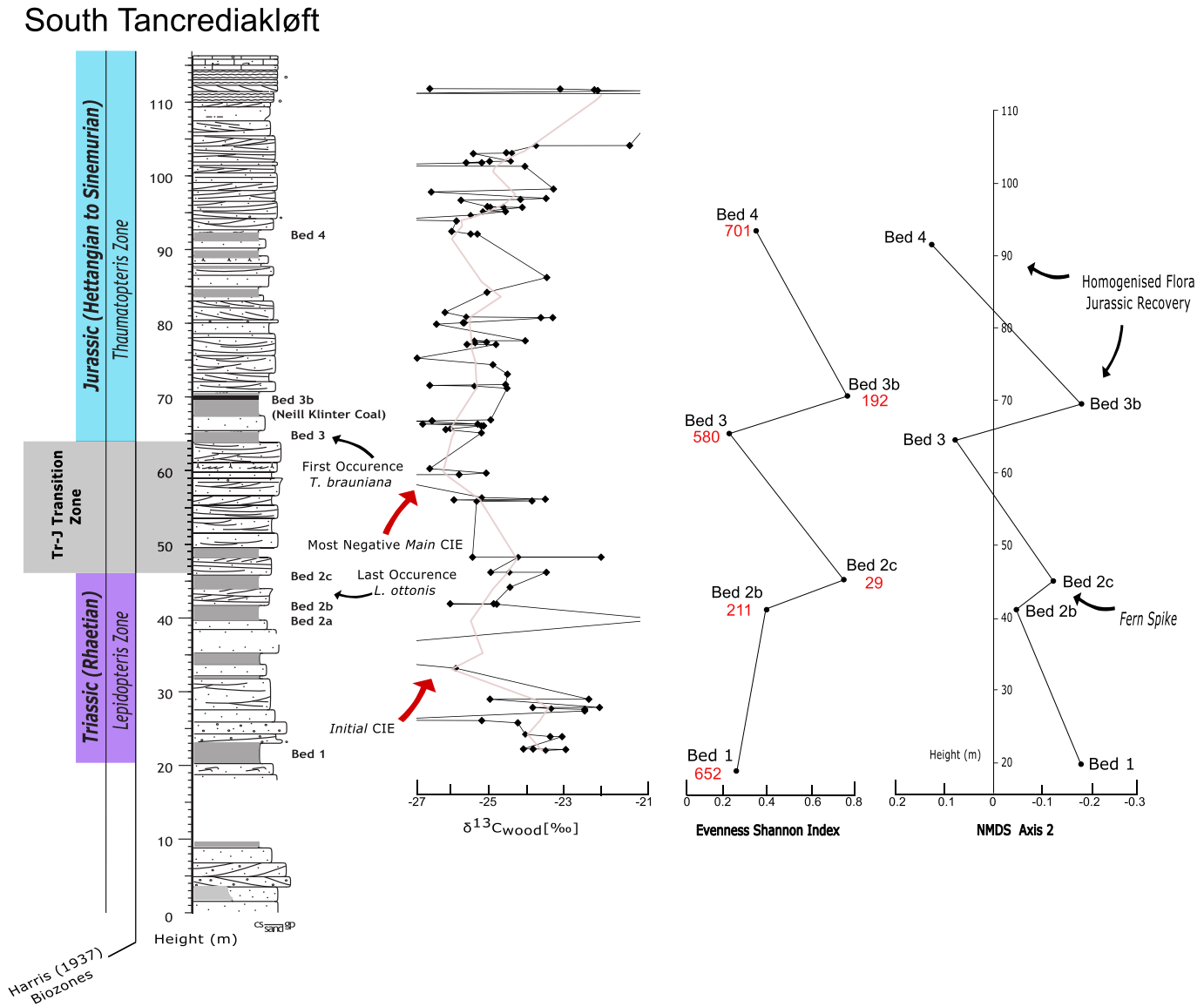

Fig. 6. Comparison of evenness, palaeoecology trends, and stable isotope stratigraphy for South Tancrediakløft plotted on depth in metres. From left to right: Stratigraphic log showing biozonation from Harris (1937) and division of the section into Triassic Rhaetian (purple), transition zone (grey) and Jurassic Hettangian (blue) and the last and first occurrence of biozone indicator taxa *Lepidopteris ottonis* and *Thaumatopteris brauniana*. Stable carbon isotope stratigraphy for South Tancrediakløft (East, Greenland) $\delta^{13}C_{wood}$ [‰] with a pink LOESS curve (0.10 fitting parameter). Evenness estimated with Shannon Index (H), red numbers beside the bed numbers indicate total macrofossil leaf occurrences per bed. For the Shannon Index H, output values range from zero to one with high values approaching one indicating absolute community evenness and low values approaching zero indicating unevenness (PAST 4, Hammer et al., 2001). NMDS axis 2 South Tancrediakløft bed values from Fig. 5 (this study) with highlighted points of biphasic disturbance (fern spike and homogenised flora). (For interpretation of the references to colour in this figure legend, the reader is referred to the web version of this article.)

to be biostratigraphically closest to Astartekløft bed 5 is bed 3 although, a compositionally equivalent bed is missing.

Our analyses demonstrate the magnitude of diversity loss scales with the pre-crisis standing diversity when comparing trends for both localities. Further, it may be that the ecologically richer succession at South Tancrediakløft, which captures a greater range of depositional environments and likely habitat types, is a better reflection of the true scale of plant diversity loss associated with the ETME. Our findings clearly show that South Tancrediakløft shares trends in ecological composition, diversity, and turnover with Astartekløft. Also, considering the $\delta^{13}C$ data (Fig. 8) we propose that the fossil and carbon isotope records at South Tancrediakløft capture a key interval for the Tr–J transition, correlating the negative CIE of ~ −3 ‰ occurring at ~34.9 m (preceding fossiliferous beds 2b and 2c) with the 'initial' negative CIE at St Audrie's Bay (Hesselbo et al., 2002) and further correlating it to the Hettangian stage GSSP section at West Kuhjoch (Ruhl et al., 2009) (Fig. 8).

This places South Tancrediakløft within the end-Triassic mass extinction global context, and supports the evident environmental disruption and floristic turnover at this locality as a response to CAMP activity. The biodiversity loss preserved in South Tancrediakløft beds 2b and 2c here correspond to the reported loss in Astartekløft beds 3 and 4.

5.2. *Strong regional signal in forest structure/canopy*

Evidence for a strong regional vegetation signal is interpretable from both palaeodiversity and palaeoecology results at South Tancrediakløft. There is a clear biphasic disturbance pattern: a flora at bed 1, a disturbance at bed 2b/2c (fern-spike), a 'transitional-like' flora at bed 3, a subsequent disturbance at bed 3b (low biodiversity), and a response: Jurassic 'recovery' flora at bed 4. An alternative interpretation of the

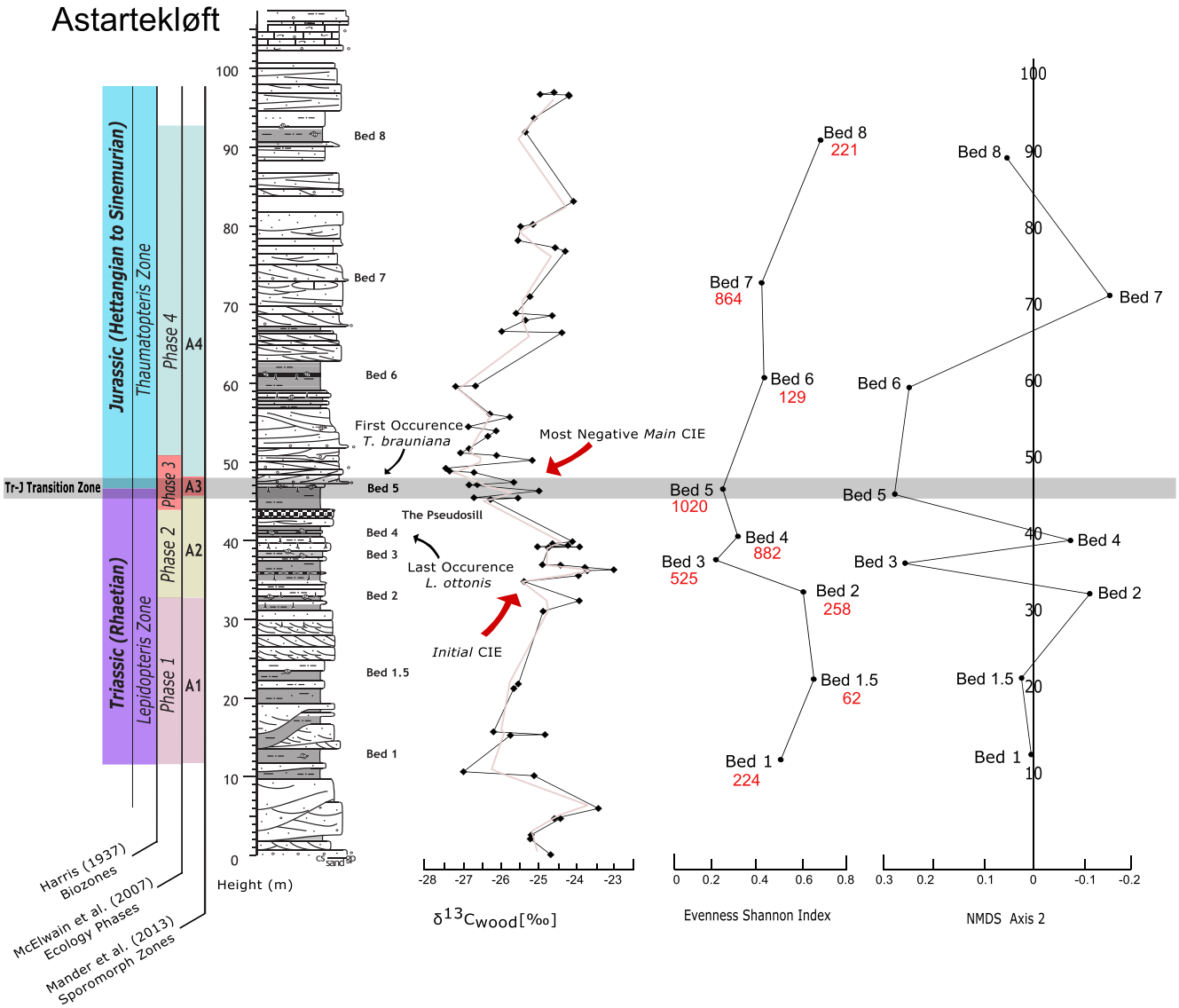

Fig. 7. Comparison of evenness, palaeoecology trends, and stable isotope stratigraphy for Astartekløft plotted on depth in metres. From left to right: Stratigraphic log showing biozonation from Harris (1937) and division of the section into Triassic Rhaetian (purple), transition zone (grey) and Jurassic Hettangian (blue), the last and first occurrence of biozone indicator taxa *Lepidopteris ottonis* and *Thaumatopteris brauniana*, and zonation from McElwain et al. (2007) (ecology zones 1–4) and Mander et al. (2013) (sporomorph assemblage zones 1–4). Stable carbon isotope stratigraphy for Astartekløft (East, Greenland) $\delta^{13}C_{wood}$ [‰] with a pink LOESS curve (0.10 fitting parameter) from Hesselbo et al. (2002). Evenness estimated with Shannon Index (H); red numbers beside the bed numbers indicate total macrofossil leaf occurrences per bed. For the Shannon Index H, output values range from zero to one with high values approaching one indicating absolute community evenness and low values approaching zero indicating unevenness (PAST 4, Hammer et al., 2001). NMDS axis 2 Astartekløft bed values from Fig. 5 (this study). (For interpretation of the references to colour in this figure legend, the reader is referred to the web version of this article.)

apparent fluctuations in richness between beds is that the patterns of change represent a taphonomic artifact. Beds with the greatest richness are lacustrine and contain the most fossils. Lacustrine environments may have the capacity to preserve more and 'better' leaf macrofossils. Lake floors may also not be as prone to post-burial erosion as crevasse splays or other floodplain deposits. South Tancrediakløft has a notably smaller sample size than Astartekløft and additional analyses may be necessary to compare the two sites proportionally.

The NMDS analysis (Fig. 5) indicates a clear palaeoecological distinction between Triassic and Jurassic beds following the Harris (1937) biozonation. The results from the two-way PERMANOVA demonstrate a significant difference between Triassic and Jurassic assemblages yet show no significance for differences between the localities; suggesting strong similarities, thus supporting regional floristic change. The three richest beds (1, 3, and 4) represent four different types of dominating flora: *Lepidopteris/Ptilozamites/Pterophyllum* dominated bed 1, *Podozamites/Pterophyllum* dominated bed 3, and bed 4 dominated by ginkgo morphotaxa (*Baiera, Sphenobaiera,* and *Ginkgoites*) and *Podozamites*.

Comparing the late Triassic and early Jurassic canopy compositions, the liana-like taxon *Lepidopteris* and seed-fern taxon *Ptilozamites* are replaced with conifer and ginkgo morphotaxa – a clear shift to an arborescent-dominated environment in the earliest Jurassic (~82 % total floristic composition). Additionally, a notable loss is seen in the lower and mid-canopy habits when comparing the flora of the uppermost Triassic beds to the lowermost Jurassic beds. A 23 % loss for mid-canopy morphotaxa (bennettites and cycads) and a 37 % loss for lower-canopy morphotaxa (ferns and lianas). At Astartekløft the loss of the

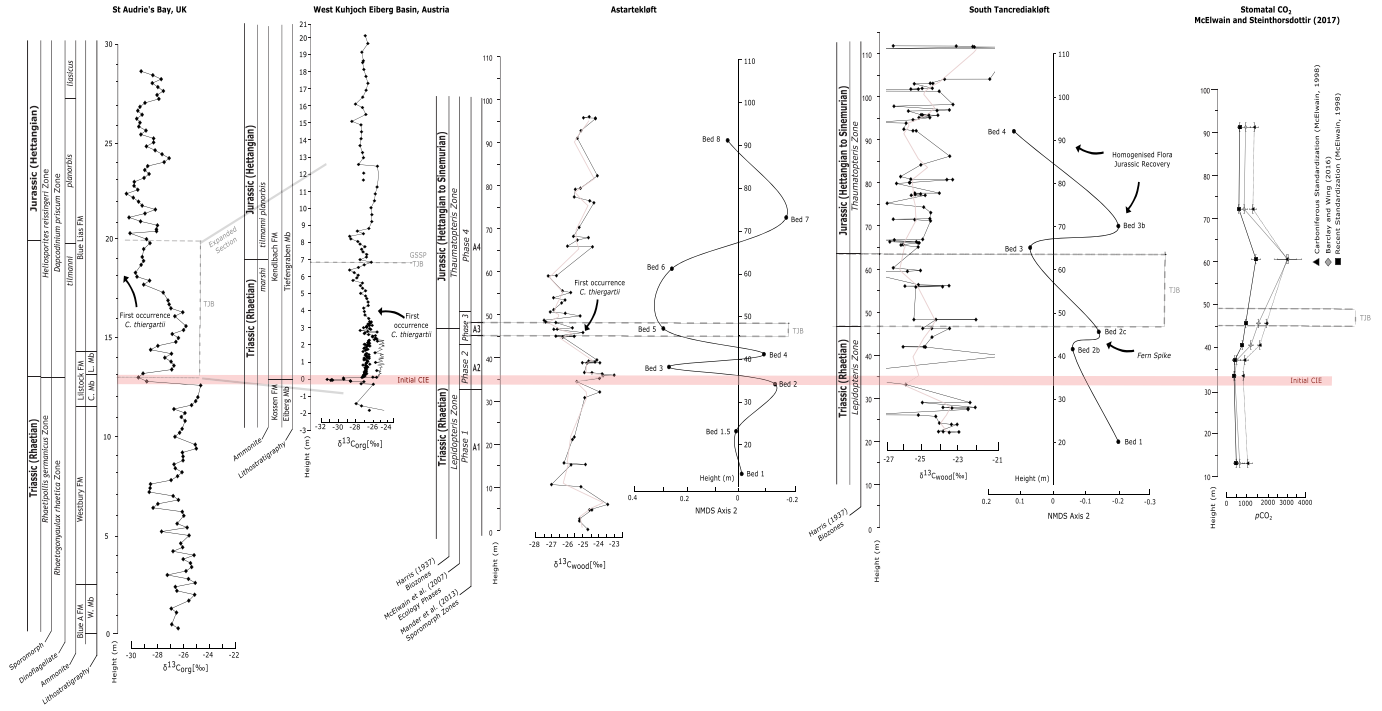

Fig. 8. Stable carbon isotope stratigraphy correlation of South Tancrediakløft ($\delta^{13}C_{wood}$) to other localities. From left to right: St Audrie's Bay (England, UK) $\delta^{13}C_{org}$ [‰] from Hesselbo et al. (2002). Kuhjoch West, Eiberg Basin (Austria) is base of Jurassic System (GSSP; Hillebrandt et al., 2013) with $\delta^{13}C_{org}$ [‰] values from the section expanded for better viewing from Ruhl et al. (2009). Astartekløft (East, Greenland) $\delta^{13}C_{wood}$ [‰] with a LOESS curve (0.10 fitting parameter) from Hesselbo et al. (2002), next to the NMDS axis 2 values from Fig. 5 (this study). South Tancrediakløft (East, Greenland) $\delta^{13}C_{wood}$ [‰] with a LOESS curve (0.10 fitting parameter), next to the NMDS axis 2 values from Fig. 5 (this study) with highlighted points of biphasic disturbance (fern spike and homogenised flora). Palaeo-CO_2 values for the Astartekløft section (across the Triassic–Jurassic transition) via the stomatal proxy from McElwain and Steinthorsdottir (2017). All sections have the 'initial' CIE indicated as well as the Triassic–Jurassic boundary (TJB), and relevant biozonation and lithostratigraphy. Occurrence of continental palynomorph marker *Cerebropollenites thiergartii* is indicated where relevant.

mid-canopy habit is described towards the end of the Rhaetian. Both the mid and lower-canopy habit at South Tancrediakløft drastically decline by the onset of the Jurassic (at beds 3b and 4). Some mid and lower-canopy morphotaxa occurrences are present in bed 3 though they are in declining numbers compared to beds 1-2c. The composition of bed 3b consists of only three arborescent morphogenera which are poorly preserved. The few mid/lower-canopy morphotaxa present in bed 4 (*Equisetites*, *Neocalamites*, *Dictyophyllum*, and *Nilssonia*) occur in low abundances. The loss of this habit may be correlated with the coal remains in bed 3b, as fire activity may have been driven by increased airflow or structural vegetation changes (Belcher et al., 2010). In addition, pCO_2 values from McElwain and Steinthorsdottir (2017) suggest elevated CO_2 levels of 1481–3018 ppm (bed 3b is positioned directly after this peak; Fig. 8). The transition to a drier and warmer regional climate in the earliest Jurassic is also suggested by the palynological record showing Hettangian sporomorph assemblages dominated by *Classopollis* pollen in Sweden (Van De Schootbrugge et al., 2009) and the UK (St Audrie's Bay; Bonis et al., 2010).

5.3. Fern spike and evidence of disturbance

Disturbances in ecosystem function caused by climatic change may be identified in the fossil record by 'fern spikes' as they play a key role in vegetation recovery (Thomas and Cleal, 2022; Azevedo-Schmidt et al., 2024). A fern spike is evident at South Tancrediakløft between beds 2b and 2c, mainly characterised by dominant morphotaxa *Dictyophyllum* and *Equisetites*. In the Mesozoic fossil record ferns are often considered 'disaster morphotaxa' (Rothwell, 1996; Husby, 2013). Reasons for these spikes are due to ferns having resilient traits, e.g. desiccation tolerance and efficient dispersal capabilities (Husby, 2013; Anderson, 2021; Thomas and Cleal, 2022). Van De Schootbrugge et al. (2009) highlight 'overwhelming' fern dominance within the Tr–J transition palynological record for Germany and Sweden and associate this with Northern Hemisphere terrestrial deforestation/ferns colonizing disturbed habitats or notable greenhouse warming causing climate change effects such as increased precipitation. The fern morphotaxa characterising the here observed spike are *Dictyophyllum*, *Marattia*, *Osmundopsis*, *Cladophlebis*, and *Todites* (Table 2), representing 68 % of bed 2b and 48 % of bed 2c. The percentage of ferns in the other beds is significantly lower (0.94 % in bed 1, 16 % in bed 3 and 3 % in bed 4). The spike seen in beds 2b and 2c indicates ecosystem disturbance and occurs directly after the negative CIE at ~34.9 m corresponding to the 'initial' negative CIE at St Audrie's Bay (discussed in Sections 4.1 and 5.1).

Generic richness assessments for South Tancrediakløft demonstrate lower richness for beds 2b, 2c, and 3b (Fig. 4). These same beds also show increased evenness (Fig. 6). Although somewhat counterintuitive, plant communities may gain evenness following an environmental disturbance if the dominant morphotaxa have an uneven distribution of resilient traits and are susceptible to the disturbance (Hillebrand et al., 2008). Thus, bed 3b is here interpreted as a 'disaster' bed like beds 2b and 2c based on its diversity results (low richness and high evenness). The low richness and high evenness of bed 3b also appears as the 'aftermath' of elevated pCO_2 (McElwain and Steinthorsdottir, 2017). The palaeoecology and palaeodiversity trends of both beds 2b/2c and 3b suggest there is a biphasic disturbance pattern at South Tancrediakløft.

5.4. Ecosystem recovery and rise of ginkgoes

Ecosystem recovery in the lowermost Jurassic beds at South Tancrediakløft is marked by the first ginkgo-fern co-occurrence (bed 4, see Table 2).

Contemporary studies of ecological succession have demonstrated

how ferns can benefit secondary succession systems. Azevedo-Schmidt et al. (2024) describe how ferns specifically increase soil moisture and stability while decreasing soil contamination – thus facilitating recolonisation following disturbance. Observing the generic richness plot for South Tancrediakløft (Fig. 4), vegetation recovery may be reflected by the significant rebound for bed 4 (increased generic richness) from the declined generic richness of bed 3b composed of only three morphotaxa (Table 2).

Another possible interpretation is increased biotic homogenisation in response to environmental disturbance (Rolls et al., 2023): Astartekløft has an overall lower generic richness than South Tancrediakløft (33 vegetative morphogenera with a sample size of 43,030 vs 27 vegetative morphogenera with a sample size of 2369) and biotic homogenisation at South Tancrediakløft increases with the occurrence of ginkgo morphotaxa (bed 3b and 4). This homogenisation is primarily characterised by reduced mid- and lower-canopy habits, causing South Tancrediakløft in the lowest Jurassic to become compositionally (and perhaps environmentally) more similar to Astartekløft.

This may be explained by the positive correlation of beta diversity and spatial environmental variability. Biotic homogenisation occurs when environmental heterogeneity decreases or increases (Rolls et al., 2023). For both localities, the Rhaetian floristic composition is clearly dissimilar to that of the Hettangian and both localities share a more homogeneous flora in the later fossiliferous Jurassic beds within both sections (bed 3b and 4 vs bed 7 and 8 at Astartekløft). This would indicate a basin-scale upper-canopy dominated Jurassic recovery flora (91.5 % total composition for Astartekløft and 82 % for South Tancrediakløft).

6. Conclusions

The macrofloristic fossil record of South Tancrediakløft shows a significant turnover initiating prior to the proposed 'main' negative CIE correlated to the previously studied sections of Astartekløft, St Audrie's Bay, and Kuhjoch, Eiberg Basin. Our study demonstrates 54 % loss in generic richness prior to the 'main' negative CIE (cf. 35 % loss in generic richness at Astartekløft), and loss of the lower and mid-canopy habits (~37 % and ~ 23 % decline respectively) by the earliest Jurassic.

We hypothesise that these ecological trends are representative of the entire Jameson Land Basin, reflecting the significant climatic and terrestrial environmental change described for the Triassic–Jurassic boundary interval (McElwain et al., 1999; Van De Schootbrugge et al., 2009; Deenen et al., 2010; Steinthorsdottir et al., 2011; Mander et al., 2013; Wignall and Atkinson, 2020; Ruhl et al., 2020).

A biphasic disturbance pattern is observed at South Tancrediakløft by fern spikes and compositional homogenisation of the Jurassic recovery flora; accompanied by high compositional evenness. Preservation of the 'initial' and 'main' negative $\delta^{13}C_{wood}$ values in the observed section support this pattern. Further, our findings highlight upper-canopy dominance (>80 % total composition) in the Jurassic for both localities. The floristic composition of our assemblage is congruent with the original Harris (1937) Rhaetian and Hettangian biozonation and supports the findings of McElwain et al. (2007) at Astartekløft, showing evidence for a regional-scale vegetation turnover across the Tr–J boundary regardless of variation in depositional environments.

The stable carbon isotopic record presented here for South Tancrediakløft stratigraphically repositions the 'initial' CIE at Astartekløft (cf. Hesselbo et al., 2002), placing the anomaly near bed 3 (~ 34.3 m), corresponding to proposed 'initial' excursion of ~ −3 ‰ at South Tancrediakløft at 34.9 m. We concur with previous work that suggests the 'main' CIE at Astartekløft (~ 48.7 m) to coincide with the 'main' CIE observed in the uppermost pre-Planorbis beds of St Audrie's Bay (~ 17.5 m) (Hesselbo et al., 2002; Mander et al., 2013) and correlate this with the South Tancrediakløft ~2 ‰ negative CIE (at ~58.5 m in the section). This positioning facilitates the correlation of the South Tancrediakløft section with the GSSP Kuhjoch, Eiberg Basin and the Triassic–Jurassic boundary. These findings clearly place South Tancrediakløft and the Jameson Land Basin within a global context, connecting this significant floristic turnover to CAMP-driven environmental disturbance. Our study broadens the collective understanding of vegetation dynamics for the Tr–J transition and stands as a primary example of the importance of census style collections.

Supplementary data to this article can be found online at https://doi.org/10.1016/j.palaeo.2025.113266.

CRediT authorship contribution statement

Antonietta B. Knetge: Writing – review & editing, Writing – original draft, Visualization, Investigation, Formal analysis, Data curation, Conceptualization. **Catarina Barbosa:** Writing – review & editing, Investigation, Formal analysis, Data curation. **William J. Matthaeus:** Writing – review & editing, Supervision, Resources, Investigation, Formal analysis. **Richard S. Barclay:** Writing – review & editing. **Ian J. Glasspool:** Writing – review & editing, Resources, Investigation. **Bernard Gomez:** Writing – review & editing, Supervision, Resources. **Stephen P. Hesselbo:** Writing – review & editing, Resources, Investigation, Formal analysis. **Mihai E. Popa:** Writing – review & editing, Resources, Methodology, Investigation. **Micha Ruhl:** Writing – review & editing, Visualization, Supervision, Resources, Formal analysis. **David Sunderlin:** Writing – review & editing, Resources, Investigation. **Finn Surlyk:** Writing – review & editing, Writing – original draft, Resources, Investigation, Formal analysis. **Jennifer C. McElwain:** Writing – review & editing, Writing – original draft, Supervision, Resources, Project administration, Methodology, Investigation, Funding acquisition, Formal analysis, Conceptualization.

Declaration of competing interest

This manuscript, *Census collection of two fossil plant localities in Jameson Land, East Greenland supports regional ecological turnover and diversity loss at the end-Triassic mass extinction*, has not been published elsewhere and it reflects original research conducted by its authors. None of the authors have any conflicts of interest to disclose concerning this study.

This project has received funding from the European Research Council, grant agreement n° 101020824.

Data availability

The authors confirm that all data necessary for supporting the scientific findings of this paper have been provided.

References

Allen, S.E., Lowe, A.J., Peppe, D.J., Meyer, H.W., 2020. Paleoclimate and paleoecology of the latest Eocene Florissant flora of central Colorado, U.S.A. Palaeogeogr. Palaeoclimatol. Palaeoecol. 551, 109678. https://doi.org/10.1016/j.palaeo.2020.109678.

Anderson, M.J., 2001. A new method for non-parametric multivariate analysis of variance. Austral Ecol. 26, 32–46. https://doi.org/10.1111/j.1442-9993.2001.01070.pp.x.

Anderson, O.R., 2021. Physiological Ecology of Ferns: Biodiversity and Conservation Perspectives.

Anderson, M.J., Crist, T.O., Chase, J.M., Vellend, M., Inouye, B.D., Freestone, A.L., Sanders, N.J., Cornell, H.V., Comita, L.S., Davies, K.F., Harrison, S.P., Kraft, N.J.B., Stegen, J.C., Swenson, N.G., 2011. Navigating the multiple meanings of β diversity: a roadmap for the practicing ecologist. Ecol. Lett. 14, 19–28. https://doi.org/10.1111/j.1461-0248.2010.01552.x.

Azevedo-Schmidt, L., Currano, E.D., Dunn, R.E., Gjieli, E., Pittermann, J., Sessa, E., Gill, J.L., 2024. Ferns as facilitators of community recovery following biotic upheaval. BioScience 74, 322–332. https://doi.org/10.1093/biosci/biae022.

Barbacka, M., Pacyna, G., Kocsis, Á.T., Jarzynka, A., Ziaja, J., Bodor, E., 2017. Changes in terrestrial floras at the Triassic-Jurassic Boundary in Europe. Palaeogeogr. Palaeoclimatol. Palaeoecol. 480, 80–93. https://doi.org/10.1016/j.palaeo.2017.05.024.

Barral, A., Gomez, B., Zorrilla, J.M., Serrano, J.M., Yans, J., Cazedebat, M., Daviero-Gomez, V., Ewin, T.A.M., Lécuyer, C., 2016. Local-scale analysis of plant community

from the Early Cretaceous riparian ecosystem of Hautrage, Belgium. Palaeogeogr. Palaeoclimatol. Palaeoecol. 443, 107–122. https://doi.org/10.1016/j.palaeo.2015.11.026.
Barrón, E., Comas-Rengifo, M.J., 2007. Differential accumulation of miospores in Upper Miocene sediments of the La Cerdaña basin (eastern Pyrenees, Spain). In: Comptes Rendus Palevol, Bioaccumulations et Bioconstructions Fossiles, 6, pp. 157–168. https://doi.org/10.1016/j.crpv.2006.12.001.
Behrensmeyer, A.K., Kidwell, S.M., Gastaldo, R.A., 2000. Taphonomy and Paleobiology.
Belcher, C.M., Mander, L., Rein, G., Jervis, F.X., Haworth, M., Hesselbo, S.P., Glasspool, I. J., McElwain, J.C., 2010. Increased fire activity at the Triassic/Jurassic boundary in Greenland due to climate-driven floral change. Nat. Geosci. 3, 426–429. https://doi.org/10.1038/ngeo871.
Bercovici, A., Wood, J., Pearson, D., 2008. Detailed palaeontologic and taphonomic techniques to reconstruct an earliest Paleocene fossil flora: an example from southwestern North Dakota, USA. Rev. Palaeobot. Palynol. 151, 136–146. https://doi.org/10.1016/j.revpalbo.2008.03.004.
Bond, A.D., Dickson, A.J., Ruhl, M., Raine, R., 2022. Marine redox change and extinction in Triassic–Jurassic boundary strata from the Larne Basin, Northern Ireland. Palaeogeogr. Palaeoclimatol. Palaeoecol. 598, 111018. https://doi.org/10.1016/j.palaeo.2022.111018.
Bonis, N.R., Kürschner, W.M., 2012. Vegetation history, diversity patterns, and climate change across the Triassic/Jurassic boundary. Paleobiology 38, 240–264. https://doi.org/10.1666/09071.1.
Bonis, N.R., Kürschner, W.M., Krystyn, L., 2009. A detailed palynological study of the Triassic–Jurassic transition in key sections of the Eiberg Basin (Northern Calcareous Alps, Austria). Rev. Palaeobot. Palynol. 156, 376–400. https://doi.org/10.1016/j.revpalbo.2009.04.003.
Bonis, N.R., Ruhl, M., Kürschner, W.M., 2010. Milankovitch-scale palynological turnover across the Triassic–Jurassic transition at St. Audrie's Bay, SW UK. J. Geol. Soc. 167, 877–888. https://doi.org/10.1144/0016-76492009-141.
Bray, J.R., Curtis, J.T., 1957. An ordination of the upland forest communities of Southern Wisconsin. Ecol. Monogr. 27, 325–349. https://doi.org/10.2307/1942268.
Burnham, R.J., 2008. Hide and go seek: what does presence mean in the fossil record. Ann. Mo. Bot. Gard. 95, 51–71. https://doi.org/10.3417/2007002.
Capriolo, M., Marzoli, A., Aradi, L.E., Callegaro, S., Dal Corso, J., Newton, R.J., Mills, B.J. W., Wignall, P.B., Bartoli, O., Baker, D.R., Youbi, N., Remusat, L., Spiess, R., Szabó, C., 2020. Deep CO2 in the end-Triassic Central Atlantic Magmatic Province. Nat. Commun. 11, 1670. https://doi.org/10.1038/s41467-020-15325-6.
Capriolo, M., Marzoli, A., Aradi, L.E., Ackerson, M.R., Bartoli, O., Callegaro, S., Dal Corso, J., Ernesto, M., Gouvêa Vasconcellos, E.M., De Min, A., Newton, R.J., Szabó, C., 2021. Massive methane fluxing from magma–sediment interaction in the end-Triassic Central Atlantic Magmatic Province. Nat. Commun. 12, 5534. https://doi.org/10.1038/s41467-021-25510-w.
Cleal, C., Pardoe, H.S., Berry, C.M., Cascales-Miñana, B., Davis, B.A.S., Diez, J.B., Filipova-Marinova, M.V., Giesecke, T., Hilton, J., Ivanov, D., Kustatscher, E., Leroy, S.A.G., McElwain, J.C., Opluštil, S., Popa, M.E., Seyfullah, L.J., Stolle, E., Thomas, B.A., Uhl, D., 2021. Palaeobotanical experiences of plant diversity in deep time. 1: how well can we identify past plant diversity in the fossil record? Palaeogeogr. Palaeoclimatol. Palaeoecol. 576, 110481. https://doi.org/10.1016/j.palaeo.2021.110481.
Clemmensen, L.B., 1980. Triassic rift sedimentation and palaeogeography of central East Greenland. Bull. Grønl. Geol. Unders. 136, 72.
Contreras, D.L., 2018. A workflow and protocol describing the field to digitization process for new project-based fossil leaf collections. Appl. Plant Sci. 6, e1025. https://doi.org/10.1002/aps3.1025.
Dam, G., Surlyk, F., 1993. Cyclic sedimentation in a large wave- and storm-dominated anoxic lake; Kap Stewart Formation (Rhaetian-Sinemurian), Jameson Land, East Greenland. In: Posamentier, H.W., Summerhayes, C.P., Haq, B.U., Allen, G.P. (Eds.), Sequence Stratigraphy and Facies Associations. Wiley, pp. 417–448. https://doi.org/10.1002/9781444304015.ch21.
Davies, J.H.F.L., Marzoli, A., Bertrand, H., Youbi, N., Ernesto, M., Schaltegger, U., 2017. End-Triassic mass extinction started by intrusive CAMP activity. Nat. Commun. 8, 15596. https://doi.org/10.1038/ncomms15596.
Deenen, M.H.L., Ruhl, M., Bonis, N.R., Krijgsman, W., Kuerschner, W.M., Reitsma, M., Van Bergen, M.J., 2010. A new chronology for the end-Triassic mass extinction. Earth Planet. Sci. Lett. 291, 113–125. https://doi.org/10.1016/j.epsl.2010.01.003.
Gómez, J.J., Goy, A., Barrón, E., 2007. Events around the Triassic–Jurassic boundary in northern and eastern Spain: a review. Palaeogeogr. Palaeoclimatol. Palaeoecol. 244, 89–110. https://doi.org/10.1016/j.palaeo.2006.06.025.
Götz, A.E., Ruckwied, K., Pálfy, J., Haas, J., 2009. Palynological evidence of synchronous changes within the terrestrial and marine realm at the Triassic/Jurassic boundary (Csővár section, Hungary). Rev. Palaeobot. Palynol. 156, 401–409. https://doi.org/10.1016/j.revpalbo.2009.04.002.
Hallam, A., Wignall, P.B., 1999. Mass extinctions and sea-level changes. Earth-Sci. Rev. 48, 217–250. https://doi.org/10.1016/S0012-8252(99)00055-0.
Hammer, O., Harper, D.A.T., Ryan, P.D., 2001. PAST: Paleontological Statistics Software Package for Education and Data Analysis.
Harris, T.M., 1926. The Rhaetic Flora of Scoresby Sound, East Greenland. Meddelelser om Grønland.
Harris, T.M., 1931. The Fossil Flora of Scoresby Sound, East Greenland, Part. 1. Cryptogams. Meddelelser om Grønland.
Harris, T.M., 1932a. The Fossil Flora of Scoresby Sound, East Greenland, Part 2. Seed Plants Incertae Sedis, 3rd ed. Meddelelser om Grønland.
Harris, T.M., 1932b. The Fossil Flora of Scoresby Sound, East Greenland, Part 3. Caytoniales and Bennettitales, 5th ed. Meddelelser om Grønland.
Harris, T.M., 1935. The Fossil Flora of Scoresby Sound East Greenland, Part 4. Ginkgoales, Lycopodiales and Isolated Frutifications, 2nd ed. Meddelelser om Grønland.
Harris, T.M., 1937. The Fossil Flora of Scoresby Sound East Greenland, Part 5. Stratigraphic Relations of the Plant Beds, 2nd ed. Meddelelser om Grønland.
Hesselbo, S.P., Robinson, S.A., Surlyk, F., Piasecki, S., 2002. Terrestrial and marine extinction at the Triassic-Jurassic boundary synchronized with major carbon-cycle perturbation: a link to initiation of massive volcanism? Geology 30, 251. https://doi.org/10.1130/0091-7613(2002)030<0251:TAMEAT>2.0.CO;2.
Hillebrand, H., Bennett, D.M., Cadotte, M.W., 2008. Consequences of dominance: a review of evenness effects on local and regional ecosystem processes. Ecology 89, 1510–1520. https://doi.org/10.1890/07-1053.1.
Hillebrandt, A.V., Krystyn, L., Kürschner, W.M., Bonis, N.R., Ruhl, M., Richoz, S., Schobben, M.A.N., Urlichs, M., Bown, P.R., Kment, K., McRoberts, C.A., Simms, M., Tomăsových, A., 2013. The global stratotype sections and point (GSSP) for the base of the Jurassic system at Kuhjoch (Karwendel Mountains, Northern Calcareous Alps, Tyrol, Austria). Episodes J. Int. Geosci. 36, 162–198. https://doi.org/10.18814/epiiugs/2013/v36i3/001.
Holland, S.M., 2003. Analytic Rarefaction 1.3.
Husby, C., 2013. Biology and functional ecology of equisetum with emphasis on the giant horsetails. Bot. Rev. 79, 147–177. https://doi.org/10.1007/s12229-012-9113-4.
Johnson, K.R., 2002. Megaflora of the Hell Creek and lower Fort Union Formations in the western Dakotas: vegetational response to climate change, the Cretaceous-Tertiary boundary event, and rapid marine transgression. In: The Hell Creek Formation and the Cretaceous-Tertiary Boundary in the Northern Great Plains: An Integrated Continental Record of the End of the Cretaceous. Geological Society of America. https://doi.org/10.1130/0–8137–2361-2.329.
Kent, D.V., Clemmensen, L.B., 1996. Paleomagnetism and cycle stratigraphy of the TriassicFleming Fjord and Gipsdalen Formations of East Greenland. Bull. Geol. Soc. Denmark 42, 121–136. https://doi.org/10.37570/bgsd-1995-42-11.
Kidwell, S.M., Flessa, K.W., 1998. The Quality of the Fossil.
Kovács, E.B., Ruhl, M., Demény, A., Fórizs, I., Hegyi, I., Horváth-Kostka, Z.R., Móricz, F., Vallner, Z., Pálfy, J., 2020. Mercury anomalies and carbon isotope excursions in the western Tethyan Csővár section support the link between CAMP volcanism and the end-Triassic extinction. Glob. Planet. Chang. 194, 103291. https://doi.org/10.1016/j.gloplacha.2020.103291.
Kump, L.R., Arthur, M.A., 1999. Interpreting carbon-isotope excursions: carbonates and organic matter. Chem. Geol. 161, 181–198. https://doi.org/10.1016/S0009-2541(99)00086-8.
Kürschner, W.M., Bonis, N.R., Krystyn, L., 2007. Carbon-isotope stratigraphy and palynostratigraphy of the Triassic–Jurassic transition in the Tiefengraben section — Northern Calcareous Alps (Austria). Palaeogeogr. Palaeoclimatol. Palaeoecol. 244, 257–280. https://doi.org/10.1016/j.palaeo.2006.06.031.
Kürschner, W.M., Batenburg, S.J., Mander, L., 2013. Aberrant *Classopollis* pollen reveals evidence for unreduced (2*n*) pollen in the conifer family Cheirolepidiaceae during the Triassic–Jurassic transition. Proc. R. Soc. B 280, 20131708. https://doi.org/10.1098/rspb.2013.1708.
Kustatscher, E., Ash, S., Karasev, E., Pott, C., Vajda, V., Yu, J., Mcloughlin, S., 2018. Flora of the Late Triassic, pp. 545–622. https://doi.org/10.1007/978-3-319-68009-5_13.
Kutzbach, J.E., 1994. Idealized Pangean climates: sensitivity to orbital change. In: Geological Society of America Special Papers. Geological Society of America, pp. 41–56. https://doi.org/10.1130/SPE288-p41.
Larsson, L.M., 2009. Palynostratigraphy of the Triassic–Jurassic transition in southern Sweden. GFF 131, 147–163. https://doi.org/10.1080/11035890902924828.
Li, L., Wang, Y., Kürschner, W.M., Ruhl, M., Vajda, V., 2020. Palaeovegetation and palaeoclimate changes across the Triassic–Jurassic transition in the Sichuan Basin, China. Palaeogeogr. Palaeoclimatol. Palaeoecol. 556, 109891. https://doi.org/10.1016/j.palaeo.2020.109891.
Lindström, S., 2016. Palynofloral patterns of terrestrial ecosystem change during the end-Triassic event – a review. Geol. Mag. 153, 223–251. https://doi.org/10.1017/S0016756815000552.
Lindström, S., 2021. Two-phased mass rarity and extinction in land plants during the end-Triassic climate crisis. Front. Earth Sci. 9. https://doi.org/10.3389/feart.2021.780343.
Lindstrom, S., Van De Schootbrugge, B., Dybkjaer, K., Pedersen, G.K., Fiebig, J., Nielsen, L.H., Richoz, S., 2012. No causal link between terrestrial ecosystem change and methane release during the end-Triassic mass extinction. Geology 40, 531–534. https://doi.org/10.1130/G32928.1.
Lindström, S., Sanei, H., Van De Schootbrugge, B., Pedersen, G.K., Lesher, C.E., Tegner, C., Heunisch, C., Dybkjær, K., Outridge, P.M., 2019. Volcanic mercury and mutagenesis in land plants during the end-Triassic mass extinction. Sci. Adv. 5, eaaw4018. https://doi.org/10.1126/sciadv.aaw4018.
Lundblad, B., 1959. 4. Rhaeto-Liassic Floras and Their Bearing on the Stratigraphy of Triassic-Jurassic Rocks. Sveriges Geologiska Undersökning and Geologiska institutet, University of Stockholm.
Mander, L., Twitchett, R.J., 2008. Quality of the Triassic–Jurassic Bivalve Fossil Record in Northwest Europe. Palaeontology 51, 1213–1223. https://doi.org/10.1111/j.1475-4983.2008.00821.x.
Mander, L., Twitchett, R.J., Benton, M.J., 2008. Palaeoecology of the Late Triassic extinction event in the SW UK. J. Geol. Soc. Lond. 165, 319–332. https://doi.org/10.1144/0016-76492007-029.
Mander, L., Kürschner, W.M., McElwain, J.C., 2010. An explanation for conflicting records of Triassic–Jurassic plant diversity. Proc. Natl. Acad. Sci. USA 107, 15351–15356. https://doi.org/10.1073/pnas.1004207107.
Mander, L., Wesseln, C.J., McElwain, J.C., Punyasena, S.W., 2012. Tracking taphonomic regimes using chemical and mechanical damage of pollen and spores: an example

from the Triassic–Jurassic mass extinction. PLoS One 7, e49153. https://doi.org/10.1371/journal.pone.0049153.
Mander, L., Kürschner, W.M., McElwain, J.C., 2013. Palynostratigraphy and vegetation history of the Triassic–Jurassic transition in East Greenland. J. Geol. Soc. 170, 37–46. https://doi.org/10.1144/jgs2012-018.
Martín-Closas, C., Gomez, B., 2004. Taphonomie des plantes et interprétations paléoécologiques. Une synthèse. Geobios 37, 65–88.
Marzoli, A., Callegaro, S., Dal Corso, J., Davies, J.H.F.L., Chiaradia, M., Youbi, N., Bertrand, H., Reisberg, L., Merle, R., Jourdan, F., 2018. The Central Atlantic Magmatic Province (CAMP): a review. In: Tanner, L.H. (Ed.), The Late Triassic World, Topics in Geobiology. Springer International Publishing, Cham, pp. 91–125. https://doi.org/10.1007/978-3-319-68009-5_4.
McElwain, J.C., Steinthorsdottir, M., 2017. Paleoecology, ploidy, paleoatmospheric composition, and developmental biology: a review of the multiple uses of fossil stomata. Plant Physiol. 174, 650–664. https://doi.org/10.1104/pp.17.00204.
McElwain, J.C., Beerling, D.J., Woodward, F.I., 1999. Fossil plants and global warming at the Triassic-Jurassic boundary. Science 285, 1386–1390. https://doi.org/10.1126/science.285.5432.1386.
McElwain, J.C., Popa, M.E., Hesselbo, S.P., Haworth, M., Surlyk, F., 2007. Macroecological responses of terrestrial vegetation to climatic and atmospheric change across the Triassic/Jurassic boundary in East Greenland. Paleobiology 33, 547–573. https://doi.org/10.1666/06026.1.
McGhee, G.R., Sheehan, P.M., Bottjer, D.J., Droser, M.L., 2004. Ecological ranking of Phanerozoic biodiversity crises: ecological and taxonomic severities are decoupled. Palaeogeogr. Palaeoclimatol. Palaeoecol. 211, 289–297. https://doi.org/10.1016/j.palaeo.2004.05.010.
Olsen, P.E., Kent, D.V., Et-Touhami, M., Puffer, J., 2002. Cyclo-, magneto-, and bio-stratigraphic constraints on the duration of the CAMP event and its relationship to the Triassic-Jurassic boundary. In: Hames, W., McHone, J.G., Renne, P., Ruppel, C. (Eds.), Geophysical Monograph Series. American Geophysical Union, Washington, D. C, pp. 7–32. https://doi.org/10.1029/136GM02.
Pálfy, J., Mortensen, J.K., Carter, E.S., Smith, P.L., Friedman, R.M., Tipper, H.W., 2000. Timing the end-Triassic mass extinction: first on land, then in the sea? Geology 28, 39–42. https://doi.org/10.1130/0091-7613(2000)28<39:TTEMEF>2.0.CO;2.
Pardoe, H.S., Cleal, C.J., Berry, C.M., Cascales-Miñana, B., Davis, B.A.S., Diez, J.B., Filipova-Marinova, M.V., Giesecke, T., Hilton, J., Ivanov, D., Kustatscher, E., Leroy, S.A.G., McElwain, J.C., Opluštil, S., Popa, M.E., Seyfullah, L.J., Stolle, E., Thomas, B.A., Uhl, D., 2021. Palaeobotanical experiences of plant diversity in deep time. 2: how to measure and analyse past plant biodiversity. Palaeogeogr. Palaeoclimatol. Palaeoecol. 580, 110618. https://doi.org/10.1016/j.palaeo.2021.110618.
Pedersen, K.R., Lund, J.J., 1980. Palynology of the plant-bearing Rhaetian to Hettangian Kap Stewart Formation, Scoresby Sund, East Greenland. Rev. Palaeobot. Palynol. 31, 1–69.
Percival, L.M.E., Ruhl, M., Hesselbo, S.P., Jenkyns, H.C., Mather, T.A., Whiteside, J.H., 2017. Mercury evidence for pulsed volcanism during the end-Triassic mass extinction. Proc. Natl. Acad. Sci. 114, 7929–7934. https://doi.org/10.1073/pnas.1705378114.
Popa, M.E., 2011. Field and Laboratory Techniques in Plant Compressions: An Integrated Approach.
Popa, M.E., McElwain, J.C., 2009. Bipinnate *Ptilozamites nilssonii* from Jameson Land and new considerations on the genera *Ptilozamites* Nathorst 1878 and *Ctenozamites* Nathorst 1886. Rev. Palaeobot. Palynol. 153, 386–393. https://doi.org/10.1016/j.revpalbo.2008.10.007.
Pryor, J.S., Gastaldo, R.A., 2000. Paleoecological Analysis of Two Early Pennsylvanian Mineral-Substrate Wetlands.
Rees, P.McA, Ziegler, A.M., Valdes, P.J., 2000. Jurassic phytogeography and climates: new data and model comparisons. In: Huber, B.T., Macleod, K.G., Wing, S.L. (Eds.), Warm Climates in Earth History. Cambridge University Press, pp. 297–318. https://doi.org/10.1017/CBO9780511564512.011.
Rolls, R.J., Deane, D.C., Johnson, S.E., Heino, J., Anderson, M.J., Ellingsen, K.E., 2023. Biotic homogenisation and differentiation as directional change in beta diversity: synthesising driver–response relationships to develop conceptual models across ecosystems. Biol. Rev. 98, 1388–1423. https://doi.org/10.1111/brv.12958.
Rothwell, G.W., 1996. Pteridophytic evolution: an often underappreciated phytological success story. Rev. Palaeobot. Palynol. 90, 209–222. https://doi.org/10.1016/0034-6667(95)00084-4.
Ruhl, M., Kürschner, W.M., 2011. Multiple phases of carbon cycle disturbance from large igneous province formation at the Triassic-Jurassic transition. Geology 39, 431–434. https://doi.org/10.1130/G31680.1.
Ruhl, M., Kürschner, W.M., Krystyn, L., 2009. Triassic–Jurassic organic carbon isotope stratigraphy of key sections in the western Tethys realm (Austria). Earth Planet. Sci. Lett. 281, 169–187. https://doi.org/10.1016/j.epsl.2009.02.020.
Ruhl, M., Deenen, M.H.L., Abels, H.A., Bonis, N.R., Krijgsman, W., Kürschner, W.M., 2010. Astronomical constraints on the duration of the early Jurassic Hettangian stage and recovery rates following the end-Triassic mass extinction (St Audrie's Bay/East Quantoxhead, UK). Earth Planet. Sci. Lett. 295, 262–276. https://doi.org/10.1016/j.epsl.2010.04.008.
Ruhl, M., Bonis, N.R., Reichart, G.-J., Damsté, J.S.S., Kürschner, W.M., 2011. Atmospheric carbon injection linked to end-Triassic mass extinction. Science 333, 430–434. https://doi.org/10.1126/science.1204255.
Ruhl, M., Hesselbo, S.P., Al-Suwaidi, A., Jenkyns, H.C., Damborenea, S.E., Manceñido, M.O., Storm, M., Mather, T.A., Riccardi, A.C., 2020. On the onset of Central Atlantic Magmatic Province (CAMP) volcanism and environmental and carbon-cycle change at the Triassic–Jurassic transition (Neuquén Basin, Argentina). Earth Sci. Rev. 208, 103229. https://doi.org/10.1016/j.earscirev.2020.103229.
Schaller, M.F., Wright, J.D., Kent, D.V., 2011. Atmospheric Pco2 perturbations associated with the Central Atlantic Magmatic Province. Science 331, 1404–1409. https://doi.org/10.1126/science.1199011.
Schaller, M.F., Wright, J.D., Kent, D.V., Olsen, P.E., 2012. Rapid emplacement of the Central Atlantic Magmatic Province as a net sink for CO2. Earth Planet. Sci. Lett. 323–324, 27–39. https://doi.org/10.1016/j.epsl.2011.12.028.
Schoene, B., Guex, J., Bartolini, A., Schaltegger, U., Blackburn, T., 2010. Correlating the end-Triassic mass extinction and flood basalt volcanism at the 100 ka level. Geology 38, 387–390. https://doi.org/10.1130/G30683.1.
Shimadzu, H., Dornelas, M., Magurran, A.E., 2015. Measuring temporal turnover in ecological communities. Methods Ecol. Evol. 6, 1384–1394. https://doi.org/10.1111/2041-210X.12438.
Spicer, R.A., 1981. The Sorting and Deposition of Allochthonous Plant Material in a Modern Environment at Silwood Lake. Silwood Park, Berkshire, England.
Spicer, R.A., Greer, A.G., 1986. Plant taphonomy in fluvial and lacustrine systems. Stud. Geol. (Knoxville) 15, 10–26. https://doi.org/10.1017/S0271164800001305.
Steinthorsdottir, M., Jeram, A.J., McElwain, J.C., 2011. Extremely elevated CO2 concentrations at the Triassic/Jurassic boundary. Palaeogeogr. Palaeoclimatol. Palaeoecol. 308, 418–432. https://doi.org/10.1016/j.palaeo.2011.05.050.
Surlyk, F., 1990. A Jurassic sea-level curve for East Greenland. Palaeogeogr. Palaeoclimatol. Palaeoecol. 78, 71–85.
Surlyk, F., 2003. The Jurassic of East Greenland: a sedimentary record of thermal subsidence, onset and culmination of rifting. GEUS Bull. 1, 657–722. https://doi.org/10.34194/geusb.v1.4674.
Surlyk, F., Clemmensen, L.B., Larsen, H.C., 1981. Post-Paleozoic evolution of the East Greenland continental margin. In: Geology of the North Atlantic Borderlands. Mem. Can. Soc. Petrol. Geol, pp. 611–645.
Surlyk, F., Hurst, J.M., Piasecki, S., Rolle, F., Scholle, P.A., Stemmerik, L., Thomsen, E., 1986. The Permian of the western margin of the Greenland Sea - a future exploration target. In: Future Petroleum Provinces of the World. American Association of Petroleum Geologists, pp. 629–659.
Surlyk, F., Alsen, P., Bjerager, M., Dam, G., Engkilde, M., Hansen, C.F., Larsen, M., Noe-Nygaard, N., Piasecki, S., Therkelsen, J., Vosgerau, H., 2021. Jurassic stratigraphy of East Greenland. GEUS Bull. 46. https://doi.org/10.34194/geusb.v46.6521.
Thomas, B.A., Cleal, C.J., 2022. Pteridophytes as primary colonisers after catastrophic events through geological time and in recent history. Palaeobiodivers. Palaeoenviron. 102, 59–71. https://doi.org/10.1007/s12549-021-00492-1.
Vajda, V., McLoughlin, S., Slater, S.M., Gustafsson, O., Rasmusson, A.G., 2023. The 'seed-fern' *Lepidopteris* mass-produced the abnormal pollen *Ricciisporites* during the end-Triassic biotic crisis. Palaeogeogr. Palaeoclimatol. Palaeoecol. 627, 111723. https://doi.org/10.1016/j.palaeo.2023.111723.
Van De Schootbrugge, B., Quan, T.M., Lindström, S., Püttmann, W., Heunisch, C., Pross, J., Fiebig, J., Petschick, R., Röhling, H.-G., Richoz, S., Rosenthal, Y., Falkowski, P.G., 2009. Floral changes across the Triassic/Jurassic boundary linked to flood basalt volcanism. Nat. Geosci. 2, 589–594. https://doi.org/10.1038/ngeo577.
Visscher, H., Looy, C.V., Collinson, M.E., Brinkhuis, H., van Konijnenburg-van Cittert, J. H.A., Kürschner, W.M., Sephton, M.A., 2004. Environmental mutagenesis during the end-Permian ecological crisis. Proc. Natl. Acad. Sci. 101, 12952–12956. https://doi.org/10.1073/pnas.0404472101.
Wignall, P.B., Atkinson, J.W., 2020. A two-phase end-Triassic mass extinction. Earth-Sci. Rev. 208, 103282. https://doi.org/10.1016/j.earscirev.2020.103282.
Wing, S.L., Strömberg, C.A.E., Hickey, L.J., Tiver, F., Willis, B., Burnham, R.J., Behrensmeyer, A.K., 2012. Floral and environmental gradients on a Late Cretaceous landscape. Ecol. Monogr. 82, 23–47. https://doi.org/10.1890/11-0870.1.
Zhou, N., Xu, Y., Li, L., Lu, N., An, P., Popa, M.E., Kürschner, W.M., Zhang, X., Wang, Y., 2021. Pattern of vegetation turnover during the end-Triassic mass extinction: trends of fern communities from South China with global context. Glob. Planet. Chang. 205, 103585. https://doi.org/10.1016/j.gloplacha.2021.103585.